

Fetal asphyxia: short and long-term consequences and its role in preconditioning

Eveline STRACKX

promotor :

dr. J. PRICKAERTS

co-promotor :

dr. D.L.A. VAN DEN HOVE

Similia Similibus curentur
'Likes are cured by likes'

Hippocrates
(460-370 BC)

Preface

This thesis is made to graduate as a master in Clinical Molecular Life sciences. While writing it, I realized that this part of my life is almost coming to an end. After approximately 4 years behind books at the transnational University Limburg, it is nearly time to graduate. Theory will be put into practice.

Of course I could not have finished my master and internship at the department 'Brain and Behavior' of Maastricht University without the good help and support of some special people. I would like to say thank you to all of them.

First I would like to thank my promotor dr. Jos Prickaerts for his guidance and counseling. I would also like to thank my copromoter and supervisor dr. Daniel Van den Hove. If it was not for him, I would not have been able to learn this much. He taught me how to think in a scientific manner. Thank you for the interest and the help. Next, my gratitude goes out to dr. Danilo Gavilanes for providing me a very nice and fascinating project, for the interesting meetings every week and for his clinical point of view. I also want to say thank you to Hellen Steinbusch for the help in the lab and to Prof. dr. Harry Steinbusch for giving me the opportunity to explore the lab.

Finally, I would like to say thank you to my family and my friend. Mama, papa and Kristine, you have been there all along. Thank you for giving me the opportunity to study and to complete this master. Thank you for giving me good advice and for always listening to me. Thank you for being my parents. Ward, thank you for always being there for me!

Thank you all for the support,

Eveline

Table of contents

PREFACE	II
TABLE OF CONTENTS	III
LIST OF ABBREVIATIONS	IV
ABSTRACT	V
1. INTRODUCTION	1
1.1 BIRTH ASPHYXIA	2
1.1.1 <i>Causes of birth asphyxia</i>	2
1.1.2 <i>Consequences of asphyxia</i>	3
1.1.3 <i>Animal models of asphyxia</i>	4
1.1.4 <i>Mechanisms of asphyxia</i>	4
1.1.5 <i>Treatment of hypoxic-ischemic encephalopathy</i>	8
1.2 HYPOXIC-ISCHEMIC PRECONDITIONING.....	9
1.2.1 <i>Hypoxic-ischemic preconditioning in adult animals</i>	9
1.2.2 <i>Hypoxic-ischemic preconditioning in the developing brain</i>	11
1.3 AIM AND HYPOTHESIS.....	12
2. MATERIALS AND METHODS	13
2.1 PART I: FETAL ASPHYXIA.....	13
2.1.1 <i>Experimental set-up and animal model</i>	13
2.1.2 <i>Morphological analysis</i>	13
2.2 PART II: HYPOXIC-ISCHEMIC PRECONDITIONING.....	18
2.2.1 <i>Experimental set-up and animal model</i>	18
2.2.2 <i>Morphological analysis</i>	20
3. RESULTS	23
3.1 PART I: FETAL ASPHYXIA.....	23
3.1.1 <i>Presynaptic bouton densities</i>	23
3.1.2 <i>Volume estimates</i>	24
3.1.3 <i>Number of synapses</i>	24
3.2 PART II: HYPOXIC-ISCHEMIC PRECONDITIONING.....	26
3.2.1 <i>Neonatal mortality</i>	26
3.2.2 <i>Birth weight</i>	27
3.2.3 <i>Body weight</i>	27
3.2.4 <i>General observations</i>	28
3.2.5 <i>TUNEL</i>	28
3.2.6 <i>Volume estimates</i>	30
4. DISCUSSION	32
4.1 <i>The long-term effect of severe fetal asphyxia</i>	32
4.2 <i>Mild fetal asphyxia and its role in preconditioning</i>	35
REFERENCES	39
APPENDIX	43

List of abbreviations

ATP	adenosine-tri-phosphate
AMPA	amino-3-hydroxy-5-methyl-4isoxazole agonists
BDNF	brain-derived neurotrophic factor
Ca	calcium
CREB	cAMP-response-element-binding protein
DAB	3,3'-diaminobenzidine tetrahydrochloride
E	embryonic day
EEG	electroencephalogram
EPO	erythropoietin
ERK	extracellular regulated kinase
FA	fetal asphyxia
GEF	guanine nucleotide exchange factor
Glu	glutamate
GMP	Guanyl-mono-phosphate
HIF	hypoxia inducible factor
K	potassium
KA	kainite
MAPK	mitogen-activated protein kinase
MEK	mitogen-activated protein kinase/extracellular regulated kinase
mFA	mild fetal asphyxia
MWM	Morris Water Maze task
Na	sodium
NF-κB	nuclear factor- κB
NMDA	N-methyl-D-aspartate
nNOS	neuronal nitric oxide synthase
NO	nitric oxide
NOS	nitric oxide synthase
OF	Open Field Test
P	postnatal day
PA	perinatal asphyxia
ROS	reactive oxygen species
RT	room temperature
sFA	severe fetal asphyxia
sPA	severe perinatal asphyxia
TBS	tris-buffered saline
TBS-T	tris-buffered saline with Triton-X100
VEGF	vascular endothelial growth factor

Abstract

Asphyctic brain injury is a common and serious problem. It is a major cause of short and long-term neurological dysfunction in children and adults. Although the last few decades the knowledge in this scientific field has improved incredibly, there are still a lot of open issues that need to be resolved.

The first part of this project investigated long-term changes in synaptic organization. Presynaptic bouton numbers and densities were analyzed, following 75 minutes of severe fetal asphyxia, induced by clamping the uterine and ovarian arteries. At the age of 19 months, fetal asphyctic animals showed a significant decrease in presynaptic bouton numbers and density in the striatum. In the fifth layer of the prefrontal cortex, on the contrary, a tendency towards an increase in presynaptic numbers was observed. Taken together, these results suggest that fetal asphyxia causes long-term, region-specific changes in presynaptic bouton numbers and density, probably by acceleration of the aging process.

The second part of this project examined whether a mild fetal asphyctic insult can provide neuroprotection against a subsequent severe perinatal insult in rat pups. Mild fetal asphyxia was induced by clamping the uterine and ovarian arteries of the pregnant dam for 30 minutes. Rat pups with or without fetal asphyxia were then subjected to severe perinatal asphyxia by immersing the uterine horns in a water bath for 18 minutes. Newborns, which underwent mild fetal asphyxia, had a tendency towards a lower mortality rate, a higher body weight and less TUNEL-positive cells in the striatum at postnatal day 8 compared to the newborns with severe perinatal asphyxia only. In conclusion, mild fetal asphyxia seemed to cause robust neuroprotection against severe perinatal asphyxia by lessening the number of delayed apoptotic cells. Therefore, down regulation of apoptotic cell death is probably one of the mechanisms involved in hypoxic-ischemic preconditioning.

1. Introduction

Birth asphyxia is a world-wide problem. It is a medical condition of severely deficient oxygen supply to the fetus or newborn child. The prevalence of moderate or severe post-asphyctic injury is 0,86 per 1000 term life birth [1]. Moreover, 60-73% of all premature newborn infants suffered from asphyxia during pregnancy or birth [2]. Birth asphyxia results most commonly from an impaired exchange of oxygen between mother en child during pregnancy or from interference with the infant's blood flow during delivery. It can lead to hypoxic-ischemic injury in all organs and systems in the body, which is associated with high morbidity and mortality, causing 23% of all neonatal deaths [3] [Fig 1]. Approximately 15% of all cases of birth asphyxia are considered moderate or severe associated with adverse outcomes, like hepatic damage and heart and renal failure [4]. Brain damage is however of most concern, because the neonatal brain is extremely vulnerable. In the developing brain, birth asphyxia can have short and long-term complications like cognitive impairment, cerebral palsy and epilepsy.

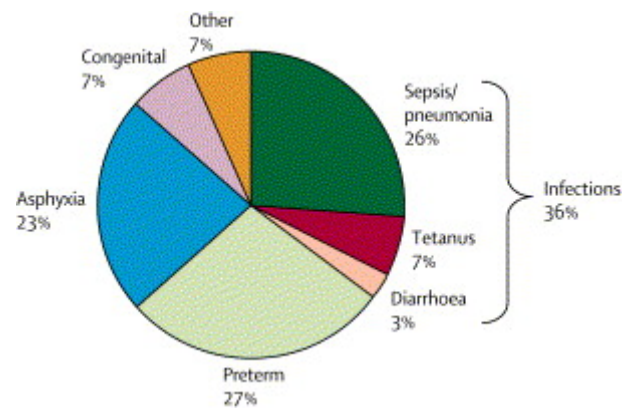


Figure 1: Estimated distribution of direct causes of 4 million neonatal deaths. These numbers were estimated for the year 2000, based on vital registration data for 45 countries and modeled estimates for 145 countries. (Reference: Lawn et al., 2005)

Although recent advances in obstetric and neonatal care have led to a great reduction in neonatal morbidity and mortality, there is still a lack of effective protective or therapeutic strategies against hypoxic-ischemic damage [5]. Improving the ability of the body's organs and systems to tolerate ischemic injury is of great importance.

A significant number of data now exists, mostly in organs like heart and kidneys, to suggest that there are intrinsic mechanisms activated in organs exposed to a hypoxic-ischemic insult, which protect them against a subsequent more severe exposure. This phenomenon is called hypoxic-ischemic preconditioning/tolerance. Less is known, however, about preconditioning in the immature brain, the main topic of this project. Consequently, defining the underlying mechanism of protection in the immature brain is an important step towards a potential therapy for improving the neurological outcome of asphyctic infants.

1.1 *Birth asphyxia*

Birth asphyxia is a medical condition resulting from deprivation of oxygen to the fetus or newborn infant long enough to cause apparent harm. Etymologically, it comes from the Greek, meaning 'pulseless'. There are two distinct time-related forms of birth asphyxia. The first one is called fetal asphyxia (FA) and occurs before birth, while the second one is called perinatal asphyxia (PA) and occurs shortly before, during or immediately after birth.

Below a critical level, deprivation of oxygen results in an impaired tissue perfusion (hypoxia) and oxygenation to the vital organs like the brain. This, in turn, leads to reduced oxygen consumption by the brain and conversion to an anaerobic metabolism with lactate as an end product, causing tissue acidosis (low pH). Simultaneously, an incomplete removal of carbon dioxide (CO₂) from the tissue takes place and a respiratory acidosis will develop, caused by abnormal high levels of CO₂ in the blood (hypercarbia) [6, 7]. In practice, the difference between 'hypoxia' and 'asphyxia' in experimental studies is its severity: generally 'hypoxia' means moderate hypoxia without metabolic acidosis, while in experimental asphyxia studies severe hypoxia is used with metabolic acidosis.

1.1.1 *Causes of birth asphyxia*

Birth asphyxia during pregnancy or birth can be defined as disturbances in the exchange of respiratory gasses between mother and child, including a reduction in the oxygen content, an elevation of the pCO₂ and a reduced pH (a combined respiratory and metabolic acidosis). It can cause hypoxic-ischemic damage, usually by an insufficient umbilical cord blood flow, a decreased uterine blood flow or to a lesser extent it may be due to an insufficient maternal arterial oxygen content and tension [Fig 2]. The most common causes are a compressed prolapsed nuchal cord, complete placental abruption, other placental lesions or severe meconium aspiration [6]. Other less common causes are intrauterine pneumonia, congenital cardiac or pulmonary anomalies, narcotic administration or, for instance, when the mother is dealing with high altitudes or when she is dealing with asphyxia herself. Asphyxia can also occur shortly after birth (PA), mainly by an obstructed airway or congenital sepsis.

A clinical diagnosis of birth asphyxia is made based on several criteria. The two main ones are a low Apgar score and evidence of an acute hypoxic event with acidemia (low blood pH). The Apgar score is a quantitative score assessed by looking at the infant's heart rate, color, responsiveness to stimulation, muscle tone and respiratory effort. For each of these 5 components, the doctor awards a maximum of 2 points for normal, 1 point for poor and 0 points for bad. An Apgar score of less than 7 at 5 minutes after birth indicates moderate neuro/cardiorespiratory depression, while a Apgar score below 3 indicates a severe depression. Hypoxia with acidemia is defined as an arterial blood pH of less than 7 and a base excess greater than 12mmol/L [8].

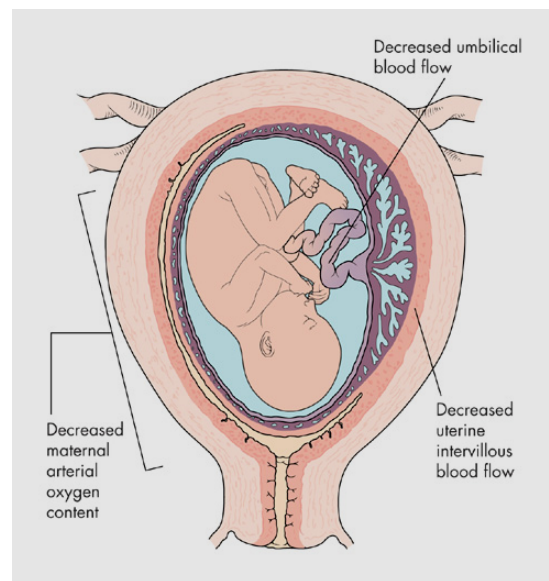


Figure 2: Possible causes of birth asphyxia. Birth asphyxia is mostly caused by a decreased umbilical blood flow, a decreased uterine intervillous blood flow or a decreased maternal arterial oxygen content.

1.1.2 Consequences of asphyxia

The impact of birth asphyxia can be somewhat variable. Some fetuses do not survive an asphyctic episode, while others survive with short-term neurological and/or behavioral changes. Examples of such changes are mental retardation, epilepsy, cerebral palsy or learning and memory deficits. Still others survive without any sign of damage [7, 9, 10]. Additionally, PA is presumed to lead to long-term neurological and psychiatric problems, developing later in adult life, like increased anxiety, decreased social exploration or impaired cognitive function in terms of relearning. A possible explanation could be that an asphyctic event accelerates or intensifies the aging process [11].

The severity of asphyxia and its neurological and behavioral consequences usually depend on the degree of acidosis, hypoxia and hypercarbia, comprising a number sensitizing factors, including severity and duration of the insult, metabolic status, cardiovascular status, gestational age and intermittency of the insult. In addition, it also depends on the cardiovascular compensatory mechanisms of the fetus. Unlike adults, fetuses have a limited capacity to increase oxygen extraction from the arterial blood. On the contrary, they are capable of redistributing their blood flow in order to preserve the circulation to organs like brain and heart. They do so by increasing the blood flow to those vital organs and decreasing the blood flow to non-vital organs like muscles and gut. According to Parer et al., also other protecting mechanisms of adaptation are changes in brain electrophysiology and behavioral status of the animal [7].

1.1.3 Animal models of asphyxia

To reveal the pathophysiology and the related mechanisms leading to hypoxic brain injury, several experimental animal models of PA and FA have evolved, using either focal or global ischemia. Focal ischemia-hypoxia, like the Rice-Vannucci model, is usually induced by the unilateral occlusion of the right carotid artery of a 7-day old pup, followed by a period of systemic hypoxia. Brain damage in focal ischemia, usually limited to the hemisphere ipsilateral to the occlusion, is characterized by selective neuronal death or infarction [12]. However, focal ischemia models differ from clinical asphyxia with respect that they lack multi-organ injury, which is present in all infants with severe asphyctic brain injury and which may influence the outcome. For that reason, we used global hypoxia-ischemia models. Global asphyxia can be provoked intrauterine by clamping the uterine and ovarian arteries of the pregnant dam or extrauterine by submersing the uterine horns, still containing the fetuses, in a water bath. In contrary to focal ischemia, global asphyxia does not produce an infarction [13, 14]. Both global procedures are explained in detail in the material and method section.

1.1.4 Mechanisms of asphyxia

Cell death

Using the above described animal models, significant advances have been made in the understanding of pathophysiological mechanisms leading to brain damage. One of the main findings is that apoptotic cell death, but not necrotic cell death, was found in several brain structures, like hippocampus, striatum and cerebellum after asphyxia [15, 16]. Apoptosis can be the result of injury caused by one of four phases occurring during hypoxia-ischemia [Fig 3]. During the primary phase, which is the actual hypoxic-ischemic event, cerebral energy failure develops, resulting in overstimulation of the neuronal glutamate receptors and primary cell death. Following reperfusion, a second phase of injury develops. There is partial recovery of cellular oxidative and metabolic processes. The reperfusion phase may be followed by a latent phase, in which there is a complete normalization of the oxidative energy metabolisms. Furthermore, this phase is characterized by low electroencephalogram (EEG) activity. In the end, the latent phase may be followed by a secondary deterioration phase, usually starting 6-15 hours after the hypoxic-ischemic event. Cerebral blood flow in this phase is markedly increased and after a while a secondary fall in cerebral blood flow occurs. The events occurring in this last phase ultimately lead to secondary or delayed apoptotic cell death [17]. All phases will be further explained in the next paragraph.

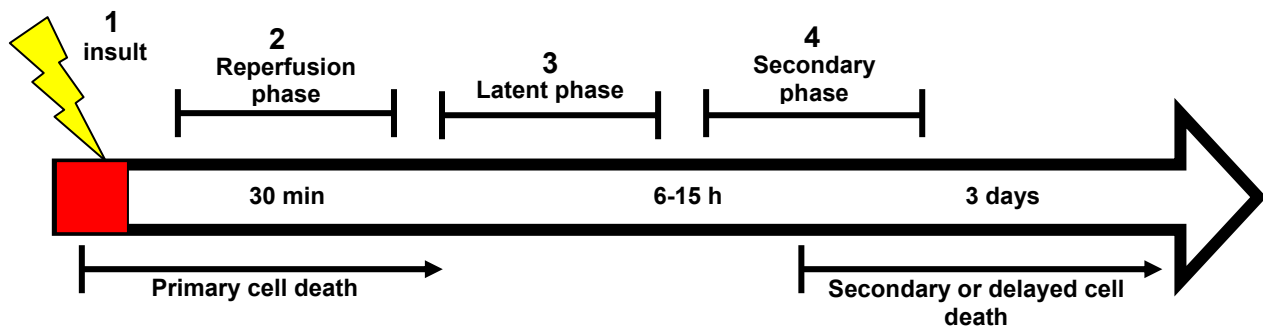


Figure 3: Different phases of hypoxic-ischemic injury. Hypoxic-ischemic insult involves 4 different phases: 1) the insult 2) the reperfusion phase 3) the latent phase 4) the secondary phase. The first two phases cause primary cell death, while the last phase causes secondary or delayed cell death. (Adapted from Gunn, 2000)

During the first phase of hypoxic-ischemic injury, cellular factors like oxidative stress, neurotransmission, Ca^{2+} concentrations and their related signaling pathways seem to play an important role [18, 19] [Fig 4]. Calcium-dependent excitotoxicity is one of the suggested mechanisms involved during the primary phase of cell death. In this cascade, the depletion of oxygen and glucose causes mitochondrial impairment and excitotoxicity, leading to delayed apoptosis. In the brain, the excitotoxicity process can take place in neurons, as well as oligodendrocytes and astrocytes. To be precise, hypoxia-ischemia leads to deprivation of the energy stores in the cell, which in turn leads to the malfunctioning of the Na^+/K^+ ATPases through lack of energy and depolarization of the cell. In the absence of a proper membrane gradient, there is an increased release and impaired uptake of glutamate, mediating a toxic buildup of extracellular glutamate in the synaptic cleft [20]. This leads to overstimulation of glutamate receptors, like the NMDA, AMPA and KA receptors in the postsynaptic membrane, inducing a lethal Ca^{2+} influx in the cell. In the cytosol, excessive Ca^{2+} amounts trigger the activation of proteases, lipases and endonucleases, which subsequently lead to cell damage and often death, while in the nucleus the overload can interfere with the transcription process [21]. Another important side effect of the high levels of Ca^{2+} is disaggregation of the microtubules, which disturbs the axonal transport system.

A second wave of injury probably takes place during reperfusion. This might be caused by the release of reactive oxygen species (ROS). ROS can trigger mitochondrial dysfunction, causing permeabilization of the outer mitochondrial membranes and leakage of mitochondrial components, like cytochrome C. Free cytochrome C can trigger the activation of an apoptotic cascade by the formation of a caspase-9-activating complex, termed an apoptosome, ultimately leading to caspase-3 activation. ROS can also trigger DNA damage, activating the tumor suppressor protein p53 to promote Bax-mediated apoptosis [6, 22].

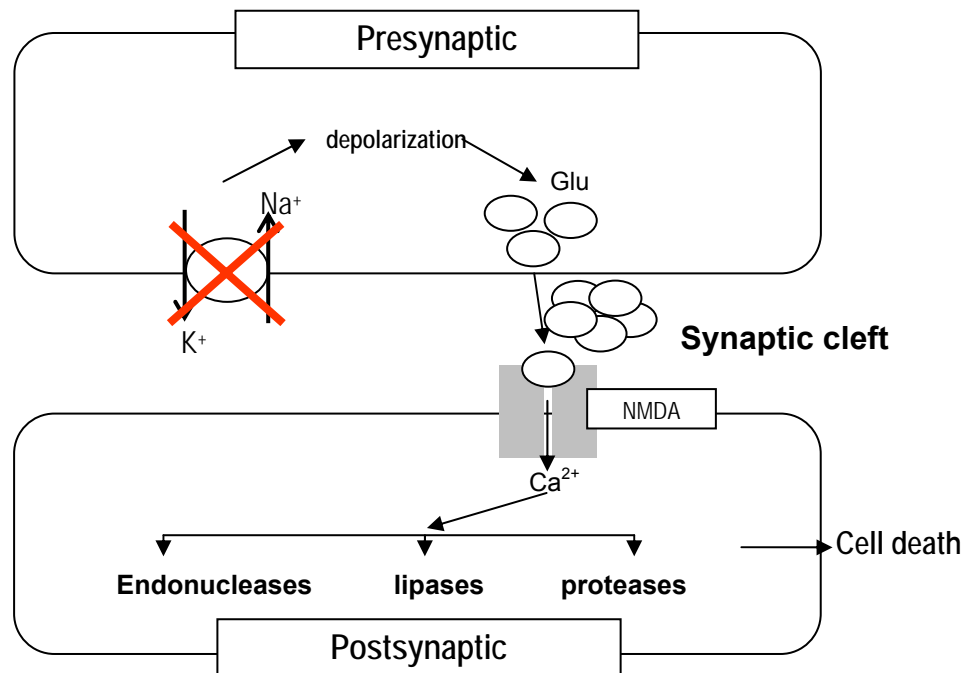


Figure 4: Schematic overview of the signaling pathway involved in the primary phase of apoptotic cell death, caused by birth asphyxia. Malfunctioning of the Na^+/K^+ ATPase causes depolarization of the cell and the release of glutamate (Glu) from the presynaptic membrane into the synaptic cleft. Glu triggers the N-methyl-D-aspartate (NMDA) receptor, which causes a calcium (Ca^{2+}) influx into the postsynaptic cell. Ca^{2+} , in turn, activates enzymes like endonucleases, lipases and proteases, that break down the cell.

Little is known, however, about the exact mechanisms leading to the delayed form of apoptosis, probably caused by the fourth phase. It is speculated that it is the result of a complex physiological cascade, which comprises many distinct events. Because dying cells are only detectable for a restricted time-window of 8-11 hours before being removed by microglia, delayed apoptosis cannot be the result of the insult or reperfusion itself [17]. The critical processes probably start as early as 6 hours after the insult [23]. They include accumulation of toxic metabolites like glutamate, overproduction of free-radicals, elevation of the expression of the Fas death receptor, caspase-8 activation, leakage and accumulation of cytosolic cytochrome C. Caspase-3 activation, showing the onset of the execution phase of apoptosis starts from 24 hours post-insult. Apoptotic cells are visible until postnatal day 15, peaking at postnatal day 8 [15, 16].

Synapse loss or formation

In other studies, neuropsychological problems associated with asphyxia, especially deficits in cognitive function have been associated with long-term alterations in the synaptic number and organization. Acceleration of the aging process and impaired cognitive function are related to a decrease in presynaptic boutons. Presynaptic boutons are enlargements of the presynaptic nerve

terminal filled with synaptic vesicles containing neurotransmitters. An electrical impulse causes fusion of those vesicles with the plasma membrane and the subsequent release of the neurotransmitters into the synaptic cleft. The number of synaptic boutons is crucial in modulating synaptic strength.

Wong et al. found a decrease in bouton density in aged rats, while Masliah et al. found a loss of synaptic input in the frontal cortex in humans comparing younger with older people [24, 25]. Although acceleration of the aging process and impaired cognitive function are reported in behavioral testing of rodents, only long-term increases in presynaptic bouton density were found in those rodents. An increase in presynaptic bouton density was found as a direct result of cerebral ischemia in a stroke model by Stroemer et al. [26]. Van de Berg et al. observed an increase in presynaptic bouton numbers in the parietal cortex and striatum of 22 month old rats, which underwent a global, perinatal asphyctic insult [14]. A possible explanation for the formation of new synaptic connections could be a compensatory mechanism for the loss of neurons to allow more neural communication. It could however not compensate for the long-term memory impairment seen in those animals, since asphyctic rats performed worse in the Morris Water Maze testing than the control animals.

Although decreases in synapse number are not reported in long-term studies, reductions in pre and postsynaptic bouton densities shortly after a hypoxic-ischemic insult (hours to days) have been reported before. Cortical neurons that survive global ischemia exhibit a reduction in dendrite complexity and loss of dendritic spines, where normally more than 90% of the synapses are found [27]. Furthermore, transient global ischemia causes a marked loss in presynaptic boutons in the chick hippocampus [28]. Similar findings have been reported in the cerebellar cortex of rats, where brief global hypoxia causes a large decrease in the density of mature presynaptic projections 1 day after the insult [29]. These results suggest that synapse loss also occurs immediately after cerebral ischemia or hypoxia.

Physiological factors

Besides neuron loss and synaptic reorganization, asphyxia can also lead to chronic damage in neurotransmission. Accordingly, Loidl et al found alterations, especially in the monoaminergic and cholinergic systems [30]. Kohlhaser et al. showed increased vesicular monoamine transporter immunoreactivity and increased vesicular acetylcholine transporter immunoreactivity [20]. Long term changes in dopamine D₁, D₂ and D₃ receptor binding were reported by Chen et al., while Gross et al. demonstrated changes in tyrosine hydroxylase, an enzyme important in the biosynthesis of catecholamines, and dopamine receptor mRNA level [31, 32]. All results described above were found in the same PA model, inducing asphyxia by immersing the uterine horns in a water bath for approximately 20 minutes.

Injury patterns

Two major patterns of brain injury are recognized in full-term neonates who suffered from asphyxia. One pattern, mostly associated with prolonged partial asphyxia, is damage to the regions of the parasagittal cortex and subcortical white matter, with relative sparing of the thalami and basal ganglia. The other pattern is a more central pattern with most of the areas affected, showing basal ganglia, thalami and cerebellum injury, with relative sparing of the cerebral cortex. Damage in the sensorimotor cortex and the hippocampus may also be present. This last pattern is mostly related to profound near term asphyxia, such as placental abruption [33, 34]. In most cases a clear distinction can be made between both types of injury, although occasionally hypoxic-ischemic brain damage shows, depending on the duration and severity of the insult, characteristics of both.

1.1.5 Treatment of hypoxic-ischemic encephalopathy

Currently, the treatment of neonates at risk for hypoxic-ischemic brain damage is only supportive, like for example blood pressure control, seizure control and assisted ventilation and medications to support the baby's breathing [35]. At the moment, there are no approved treatments that improve the neurological outcomes of those infants. However, many different treatment options have been or are currently under investigation [36-38]. The list of potential treatments is given in table 1. Although these drugs or interventions seem to ameliorate the brain injury in animal models, clinical trials have not been that successful. Only hypothermia multicentre randomized trials seemed to improve the outcome of some of the asphyctic infants. Gluckman et al. reported that head cooling was beneficial only in infants with less severe EEG changes compared to conventional care [39]. A decrease in death or moderate/severe disability from 62% in the control group to 44% in the group with whole-body hypothermia was demonstrated by Shankaran et al [40].

Table 1: List of potential treatments.

<i>List of potential treatments for hypoxic-ischemic encephalopathy</i>
Hypothermia
Fluid restriction
Hyperventilation
Anti-oxidants/oxygen free radical scavengers, e.g. vitamin K
NO/NOS inhibitors, eg Allopurinol
Calcium channel blockers, e.g. flunarizine
Corticosteroids
Magnesium sulphate
Mannitol
Opiate antagonists, e.g. naloxone
Prohylactic anticonvulsants, e.g. phenobarbitone
Membrane stabilizing agents, e.g. monoganglioside GM-1
Glutamate antagonists, e.g. MK-801 (NMDA receptor antagonist)
Anti-inflammatory agents, e.g. IL-1 β antagonist
Growth factors/anti-apoptotic factors, e.g. TGF- β

(Adapted from Vannucci et al., 1997; Dammann et al. 2000; Volpe 2001; Gluckman 2001)

It is important to note that the first hour after asphyxia represents a potential target for intervention, because this timeframe is situated prior to the final execution phase of delayed apoptotic cell death, seen 8 days after the insult. An interesting approach that may improve the outcome of birth asphyxia is to investigate the effects of the concept of hypoxic-ischemic preconditioning. Recent studies show that some stressors like a minor form of hypoxia can protect against a subsequent hypoxic-ischemic insult. Therefore, understanding the protective signaling pathways involved in hypoxic-ischemic preconditioning/tolerance and identification of drugs that mimic this protective response represents important steps towards improving the outcome of infants at risk for hypoxic-ischemic injury.

1.2 *Hypoxic-ischemic preconditioning*

Practically any stimulus capable of causing injury to a tissue or organ can, when applied close to the threshold of damage, activate endogenous protection mechanisms. Thus, it can lessen the impact of a subsequent more severe stimulus. This concept of protection against a potentially recurring challenge can also be applied to asphyxia. The phenomenon is termed 'hypoxic-ischemic preconditioning' or 'hypoxic-ischemic tolerance'. There are two temporally and mechanistically distinguishable forms of preconditioning observed in the brain, namely acute and delayed preconditioning. The first one is mediated by post-translational modification (for example phosphorylation of existing proteins by certain kinases) of proteins and is short-lived, while the second one is mediated by new protein synthesis, and can sustain for days or even weeks. Hypoxia and ischemia can induce both forms. This study focuses on the delayed form.

1.2.1 *Hypoxic-ischemic preconditioning in adult animals*

Primarily adult rodent data show that short periods of cerebral hypoxia or ischemia, inadequate to produce brain damage can provide protection against a subsequent, more severe hypoxic-ischemic insult [41]. Although a lot of research is done the last decade, the exact mechanisms underlying this preconditioning phenomenon still have to be identified.

Both in vitro and in vivo studies show that factors like the up-regulation of the glucose transporter-1 (GLUT-1), the modulation of the genomic response and the protein synthesis and the increased expression of the pro-survival inhibitor of apoptosis are related to ischemic tolerance. Other factors playing a role are the increased expression of nitric oxide – cyclic GMP, the down regulation of the glutamate receptor 2 and the induction of heat shock protein 70 [42-44].

A proposed mechanism causing neuroprotection, comprising a lot of the factors above, is the activation of the NMDA receptor [Fig. 5] [45]. The NMDA receptor is coupled to neuronal nitric oxide synthase (nNOS) via a scaffold protein. This protein couples the influx of Ca^{2+} to the activation of nNOS, leading to the production of nitric oxide (NO), which, in turn, can cause the

activation of Ras and subsequently also of kinases, like Raf, mitogen-activated protein kinase/extracellular regulated kinase (MEK) and extracellular regulated kinase (ERK). Activation of this cascade leads to the synthesis of new proteins. It is not known exactly which of the transcriptional elements are activated by this pathway, but cAMP response element binding protein (CREB) is a good potential candidate, because it can activate genes like the anti-apoptotic and pro-survival gene, Bcl-2, and the plasticity growth factor genes, brain derived neurotrophic factor (BDNF) and insulin. Other potential candidates are nuclear factor- κ B (NF- κ B) and hypoxia inducible factor-1 (HIF-1). The first one is an inducible transcription factor playing an important role in cellular survival and apoptosis, like activation of the inhibitor of apoptosis proteins, while the second one is important for inducing genes that participate in angiogenesis, vasodilation and energy metabolism [45, 46]. Examples of HIF-1 inducible genes are vascular endothelial growth factor (VEGF) and erythropoietin (EPO), which are known to be upregulated during hypoxia or ischemia.

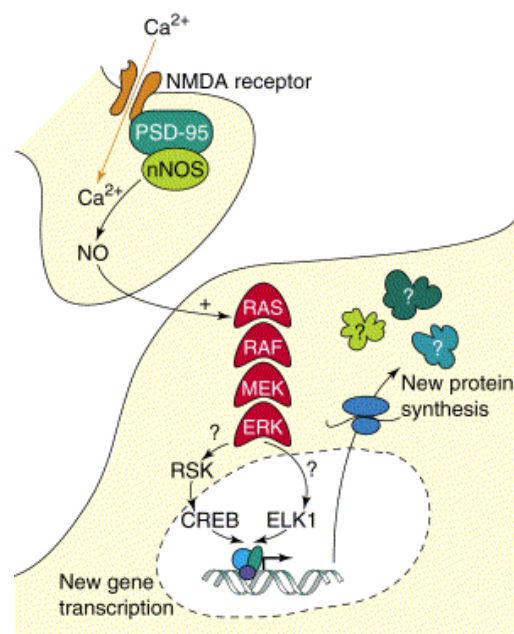


Figure 5: A schematic overview of a potential signalling cascade of neuronal ischemic preconditioning. The NMDA receptor is coupled to neuronal nitric oxide synthase (nNOS) via the scaffolding protein PSD-95, which couples Ca^{2+} influx with nNOS activation and nitric oxide (NO) production following NMDA receptor stimulation. NMDA receptor stimulation leads to NO-induced activation of p21^{Ras} (RAS), perhaps through a redox-sensitive mechanism or through activation of a NO-dependent guanine nucleotide exchange factor (GEF). Subsequently, the kinases RAF, MEK [mitogen-activated protein kinase (MAPK)/extracellular regulated kinase (ERK)] and ERK are activated. Inhibition of any of these steps during the preconditioning event is sufficient to prevent preconditioning. It is not known which transcriptional elements are activated or which protein(s) mediate tolerance; however, ELK1 and cAMP-response-element-binding protein (CREB) are attractive potential transcriptional candidates. (Reference: Dawson et al., 2000)

1.2.2 Hypoxic-ischemic preconditioning in the developing brain

The above described findings have all been found in adult animal models. Less attention has been paid to preconditioning in the developing animal brain. Gidday et al. was the first who showed that exposure of 7-day-old pups to hypoxia alone (8% oxygen for 3 hours), induced neuroprotection in the immature brain against a stroke 1 day later [47]. It was a very strong protection, meaning that a majority of the animals had no brain injury at all. Other studies with similar neonatal animal models show also neuroprotection, but less robust. They only found a reduction in brain tissue damage in preconditioned immature animals. Accordingly, Cai et al. found a reduced brain infarction size, reduced neuronal injury and increased neuronal survival 24h after a secondary hypoxic-ischemic insult [41]. Similarly, Gustavsson et al. reported that preconditioning reduced brain damage by 72%, even up to 8 weeks after induction and Xiao et al. showed a decreased caspase-3 activation [48, 49]. Additionally, it provided long-term improvement of sensimotor and spatial/cognitive functions [41, 50].

Although the mechanisms of hypoxic-ischemic preconditioning in immature animals remain to be elucidated, several essential aspects have already been described. A first aspect is that preconditioning in those neonatal animals appears to be dependent on the synthesis of new RNA and new proteins, since protein synthesis blockers can inhibit the preconditioning [51, 52]. Thus, an increased transcription and translation is necessary for the induction of hypoxic-ischemic tolerance in the neonatal brain. An increased transcription of following genes was found: VEGF, EPO and GLUT-1. They can all be induced by HIF-1 [53]. A second aspect is that the NMDA receptor may also be involved in the induction of hypoxic-ischemic tolerance. Some NMDA receptor antagonists inhibit preconditioning, while others did not block. A possible explanation could be that NMDA receptor mediates ischemic, but not hypoxic preconditioning. A third aspect playing a role is NO and NOS. A reduced NO production is involved in prenatal tolerance, given that a NO synthase inhibitor attenuated the ischemic brain injury [49].

Although some events causing the injury in neonates, involving excitotoxicity, new protein synthesis and apoptosis, are similar to those described in the adult brain, no comparison can be made because injury is age-dependent. Compared to an adult brain, the immature brain is particularly vulnerable because of its high rate of oxygen consumption, low concentrations of anti-oxidants and enhanced expression of the glutamate receptor [54]. Furthermore, apoptotic elements, like capase-3 are also upregulated in the neonatal brain [46]. Another important difference is that the immature brain is more plastic than the adult one, indicating that damage during this developmental period can have severe consequence later in life.

1.3 *Aim and hypothesis*

Birth asphyxia is a serious problem, causing world-wide thousands of victims each year. Depending on the severity and the duration of the insult these children can develop disorders like cerebral palsy and cognitive impairment. Even though during the last decade animal models have increased our understanding of the processes causing hypoxic-ischemic injury and hypoxic-ischemic preconditioning, no pharmacological treatment is available yet. Therefore this project is subdivided into 2 separate studies. The first study is intended to expand the current knowledge about the mechanisms underlying long-term hypoxic-ischemic damage, while the second study is trying to elucidate the mechanisms that induce ischemic tolerance in immature animals.

Previous work done within this group demonstrated that severe fetal asphyxia (sFA) can have serious implications for the rat brain and behavior. sFA rats undergo behavioral change compared to their healthy counterparts. At the age of 19-months they show anxiety-related behavior and cognitive impairment. Therefore the first study of this project is to continue this study by looking for alterations in synapse numbers and densities, which could be associated with the altered behavior. We hypothesize a significant loss of synapses in the prefrontal cortex and the striatum of the sFA rats compared to sham-operated rats.

The second study of this project handles hypoxic-ischemic preconditioning in the immature rat brain. This part investigates if mild fetal asphyxia (mFA) can prevent or improve the consequences of severe perinatal asphyxia (sPA) by reducing the delayed apoptotic cell death in brain structures like the striatum, normally very vulnerable for asphyxia. We hypothesize that fetal asphyctic pups are more resistant to a perinatal insult when compared to perinatal asphyctic pups not subjected to an antenatal insult. The results of this last study may have a significant contribution to the birth asphyxia research field, because identification of the cascades and factors responsible for preconditioning might provide the proper knowledge for developing novel therapeutic strategies for the treatment and/or the prevention of asphyctic brain injury in neonates.

2. Materials and methods

2.1 Part I: Fetal Asphyxia

2.1.1 Experimental set-up and animal model

Animals

For the preconditioning model timed pregnant Lewis rats were used. The inbred rats were housed individually at the Maastricht University facility for experimental animals. The animals were kept under standard laboratory conditions with water and food were given *ad libitum* and, with 12 hours dark/ 12 hours (from 7 until 7) light in a temperature-controlled environment ($21\pm 1^\circ\text{C}$). All experiments were approved by the Animal Ethics Board (Dierenexperimenten Commissie) of the University of Maastricht on animal welfare according to Dutch governmental regulations and all efforts were made to minimize the number of rats used and to minimize the pain and stress levels experienced by the animals.

Severe fetal asphyxia

At embryonic day 17 (E17), pregnant Lewis rats were anaesthetized by xylazine (1mg/kg s.c.) and ketamine (50 mg/kg i.m.). Dams were subjected to a midline laparotomy to expose both uterine horns. Severe FA was achieved by completely clamping both the uterine and the ovarian arteries with removable clamps. In the mean time, the uterine horns were kept wet, by rinsing them with a saline solution. After 75 minutes the clamps were removed to allow perfusion again. Then, the uterine horns were placed back intra-abdominally and the abdominal wall was repaired [41, 49]. Other sham pregnant rats underwent the same procedure except for the clamping of the uterine and ovarian arteries.

2.1.2 Morphological analysis

Perfusion and tissue preparation

At 19 months, rats (n=5 for each group) were anaesthetized with sodium pentobarbital (60mg/kg i.p.; Nembutal®) and sacrificed by transcardial perfusion, first with a flush of tyrode (0,1M), followed by the ice-cold 4% paraformaldehyde in 0,1M phosphate buffer (pH 7,6; room temperature (RT)). The brains were dissected rapidly from the skull and post-fixed for 24h in cold 4% buffered paraformaldehyde. For cryo-protection, the brain tissue was transferred to 30% sucrose/0,1M TRIS-buffered saline (TBS) at 4°C for 48h. To preserve the brains, they were quickly frozen and stored at -80°C until further processing. Using a cryostat (Leica CM 350, Germany), the brains were cut at -30°C into 30µm thick coronal sections.

Synaptophysin immunohistochemistry

To investigate differences in presynaptic bouton density and numbers, a synaptophysin immunostaining was executed. Synaptophysin is an integral membrane protein located in the synaptic vesicles and therefore a good marker to detect nerve terminals. All immunohistochemical reactions were carried out in a free-floating manner. They were processed simultaneously to guarantee identical conditions. All washing and dilutions steps of the antibodies were done by TBS (0,01M) with 0,2% Triton-X-100 (TBS-T). In order to minimize the background staining, all sections were pre-incubated with 5% normal goat serum (Sigma, The Netherlands) at RT for 30 minutes. Furthermore, normal goat serum (2,5%) was added to all solutions containing antibodies.

A monoclonal antibody against synaptophysin (Boehringer-Mannheim, Germany), a presynaptic protein, was used overnight at a dilution of 1:35 at 4°C. After washing, the sections were immersed in a dilution of 1:150 goat anti-mouse IgG for 1h RT. This step was followed by a monoclonal mouse anti-peroxidase antibody (1:50) with 5µg/ml horseradish peroxidase, again for 1h at RT. After several washes, the tissue slices were incubated in 0,3% 3,3'-diaminobenzidine tetrahydrochloride (DAB) in TBS-T for 15 minutes. At the same time, H₂O₂ was added to the DAB solution. All sections were washed a last time. After the labeling procedures, they were mounted on gelatine-coated glass slides and air-dried. Subsequently, the sections were dehydrated in ascending ethanol concentrations, cleared with xylene and cover-slipped with depex.

Quantitative analysis of synaptophysin staining

In this study, presynaptic bouton densities were analyzed in 2 different areas: the frontal cortex and striatum. Delineation of the different areas occurred according to Paxinos and Watson (1986).

The prefrontal area was defined between interaural 11.20 mm (anterior boundary) and interaural 7.20 mm (posterior boundary). The medial boundary consisted of a line drawn from the dorsal tip of the left brain to the top of the corpus callosum. As a lateral boundary, a line from the ventral tip of the lateral ventricle to the top of the cortex in a specific angle of 45°C was taken [14]. Measurements were performed for each of the six cortical laminae, in two adjacent areas of 5000µm². [Fig 6]

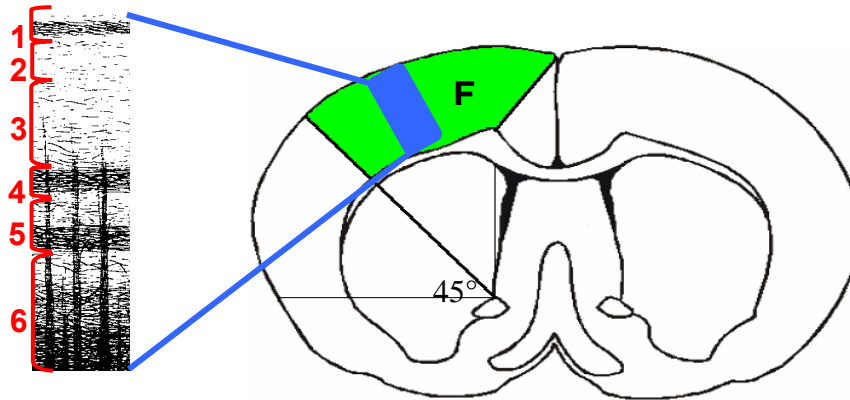


Figure 6: Delineation of the prefrontal cortex. Drawing of coronal sections through the rat brain (according to Paxinos and Watson, 1986), showing the region of frontal cortex (FC) considered in the present study (green) with the 6 cortical layers. The medial boundary of the frontal cortex consisted of a line drawn of the dorsal tip of left brain to top of corpus callosum. The lateral boundary consisted of a line drawn from the ventral tip of the lateral ventricle to the top of the cortex in a specific angle of 45° .

The striatum could be defined with unambiguous anatomical boundaries [Fig 8]. The level at which the corpus callosum first crosses the midline (10.6 mm anterior of the interaural line) was used as anterior boundary and whereas the level were the fornix joins the diencephalon (8.2 mm anterior of the interaural position) was used as posterior boundary. Dorsal and lateral boundaries were defined by the corpus callosum. The lateral ventricle defines the medial edge, and arbitrary ventral boundary consisted of a line drawn from the ventral tip of the lateral ventricle to the rhinal fissure, including a part of the nucleus accumbens [14]. To analyze the presynaptic bouton density the striatum was separated in four distinct regions: dorsal, ventral, medial and lateral, according to the construction lines in figure 7. Measurements were performed in those 4 areas in two adjacent areas of $5000\mu\text{m}^2$.

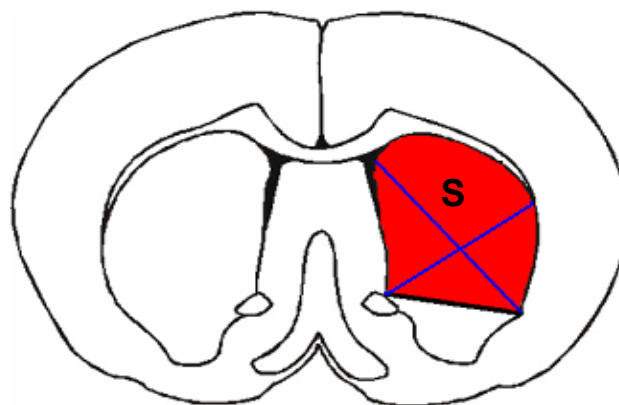


Figure 7: Delineation of the striatum. Drawing of coronal sections through the rat brain (according to Paxinos and Watson, 1986), showing the striatum (S), considered in the present study (red) with the 4 areas for measurements (blue lines). The corpus callosum defines the dorsal and lateral boundaries of the striatum. The lateral ventricle defines the medial edge, and an arbitrary ventral boundary consisted of a line drawn from the ventral tip of the lateral ventricle to the rhinal fissure, including part of the nucleus accumbens.

The immunoreactive punctae were estimated by calculating the density of the synaptophysin-immunoreactive presynaptic boutons, like previously described by Van de Berg et al [14]. Briefly, the stained sections were analyzed using the Olympus AX-70 microscope, equipped with a 100x oil immersion planachromatic objective and a 10x projection lens. For each subregion, photos were taken from two randomly chosen areas at magnification x100 using a Olympus F-view cooled CCD camera. Three different sections of each animal (interaural 10.20mm, 9.48mm and 7.84mm) were analyzed in the above described areas, yielding 36 photos for the prefrontal cortex and 24 photos for the striatum of each animal.

The synaptic punctae were detected, using the image analyzing system Cell^P. All measurements were performed at a single focal plane. A shading correction was carried out by the software, before the measurements were done, to correct for irregularities in illumination. Using a trial and error method, the threshold values, providing the most accurate measurement compared to direct visual counting were selected. Once the ideal threshold value was found, it was saved in the computer program and kept the same for all measurements (prefrontal cortex and striatum). All blood vessels and cell bodies and cortical tissue out of focus were excluded.

From these data, the density of the synaptophysin-immunoreactive presynaptic boutons was calculated for each layer of the cortex and for all 4 regions of the striatum. The data were also pooled together to a single value, referred to as cortex or striatum.

Stereological analysis: volume estimates

For stereological analysis, brains of 5 rat pups of each group (sFA en sham) were used. Brain tissue was entirely cut to serial, 30 μ m-thick coronal sections. Every 10th section was mounted on gelatinized glass slides, yielding about 12 sections per animal. Sections were dried, defatted with a Triton-X100 solution and stained with cresyl violet for the detection of Nissl body in the cytoplasm of neurons (0.01%, 11 min). Slides were coverslipped with DePeX.

Estimates of the volumes of the striatum and the prefrontal cortical layers were calculated according to the Cavalieri's principle [55]. This principle gives an unbiased estimate of the volume of the region of interest by multiplying the sum of the profile areas of all sections with the distance between the sections. To do so, a cut through the region of interest is required. The profile areas of the sections through the region of interest can be measured by tracing the boundaries of that region on video images displayed on a computer, and let the software calculate the profile area [56]. (*Schmitz et al., 2005*) The prefrontal cortex and the striatum were delineated according to the lines drawn in figure 6 and 7. Tracing was carried out with a stereology workstation and Stereoinvestigator software (MicroBrightField, Williston, VT)

Calculation of the presynaptic bouton numbers

For both the cortex and the striatum, presynaptic bouton numbers were calculated by multiplying the individual density data with the corresponding volume data, not taking into account the dimensions of the investigated parameters (i.e. $1/\mu\text{m}^2$ for density and mm^3 for volume). These numbers are not unbiased because the densities were analyzed in two dimensions (= one focal plane) instead of three dimensions. Therefore, it is not possible to calculate the exact total number of synapses, since size, shape and geometric orientation of the presynaptic boutons are unknown [57].

Statistical analysis

For each experimental group mean and SEM were calculated for all investigated parameters (presynaptic bouton density, volume and number of synapses). Comparisons between the groups were tested with a Student's *t*-test. The level of significance was set at $P < 0.05$, while a *p*-value between 0,1 and 0,05 was considered to tend towards significance (borderline significance). All calculations were performed using standard statistical software (SPSS 12.0 software)

2.2 Part II: Hypoxic-ischemic preconditioning

2.2.1 Experimental set-up and animal model

Animals

All animal experiments described below were approved by the Animal Ethics Board of the University of Maastricht on animal welfare according to Dutch governmental regulations and all efforts were made to minimize the number of rats used and their suffering. Pregnant Wistar rats (Charles River, Maastricht, The Netherlands) were delivered on day 14 of gestation. They were housed individually at the University of Maastricht facility for experimental animals. The animals were kept under standard laboratory conditions (21±2°C ambient temperature, a 12-h light/dark schedule (from 7 until 7), background noise provided by a radio, and food and water ad libitum).

Preconditioning model and study groups

A new rat model for global hypoxic-ischemic preconditioning was applied as a combination of two previously well described models. A model for mild fetal asphyxia (mFA) is used as a first hit at embryonic day 17 [41], while a model for severe perinatal asphyxia (sPA) is used as a second hit at embryonic day 21 or 22 [14] [Fig 8 and table 2].

Table 2: Experimental groups, age of intervention and abbreviations.

<i>Experimental group</i>	<i>Age of intervention</i>	<i>Abbreviation</i>
Fetal asphyxia	E17	mFA
Control caesarean delivery	E21/22	CCD
Severe perinatal asphyxia	E21/22	sPA
Mild fetal ashyxia + severe perinatal asphyxia	E17 + E21/22	mFA+sPA

Both models mimic the conditions resulting in global asphyxia during pregnancy or birth. Four groups of dams were used: mFA (n=11), sPA (n=7), mFA combined with sPA (mFA+sPA) (n=11) and the control caesarian delivery (CCD) (n=7) [Table 3]. Pregnant rats were randomly assigned to an experimental group. Exclusively male offspring were used (except for the calculation of the mortality rates), because both morphological and behavioral evidence show a differential vulnerability to a birth insult in males versus female rats. A greater impact is seen in the male gender, probably due to a protecting role of the circulating oestrogens inducing monoamine alterations and/or the sexually dimorphic nigrostriatal dopamine system [58-60]. Of note, the stage of neural development of a term rat can be compared to a preterm to very preterm human baby [61].

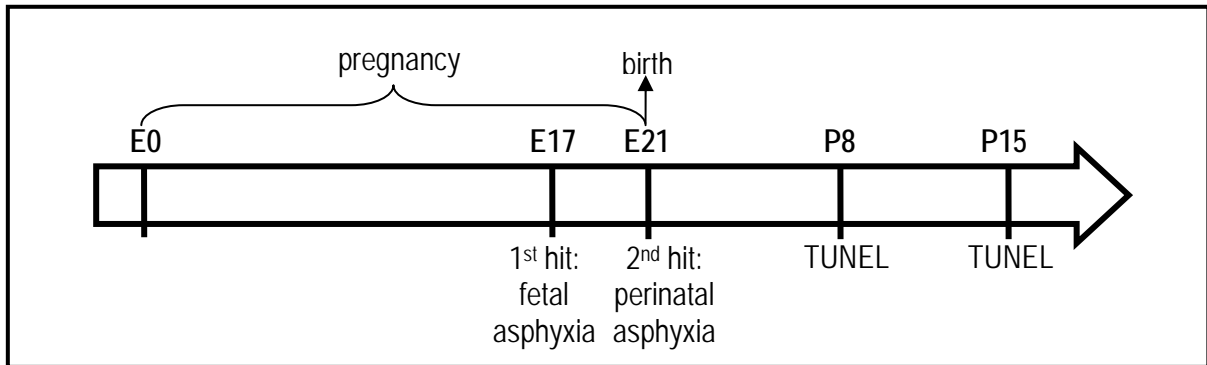


Figure 8: Scheme of experimental procedures of the preconditioning model. At E17 rats were subjected to a fetal asphyctic insult. The perinatal insult was induced at E21. Cell death was analyzed, using a TUNEL staining, at P8 and P15. (E = embryonic day; P = postnatal day)

Fetal asphyxia

At embryonic day 17 (E17), 11 pregnant Wistar rats were anaesthetized by isoflurane. Induction was done by 4% isoflurane, followed by the maintenance period with 2% isoflurane. The animals were shaved and Visagel® was applied to their eyes. To prevent hypothermia, all procedures were done within a controlled environment (37°C, 60-80% humidity, room air). Rats were subjected to a midline laparotomy to expose both uterine horns. mFA, in stead of the sFA described in the first part, was achieved by completely clamping both the uterine and the ovarian arteries with removable clamps [Fig 9]. In the mean time, the uterine horns were kept wet, by rinsing them with a saline solution. After 30 minutes (in stead of the 75 minutes used in the first study) the clamps were removed to allow perfusion again. Then, the uterine horns were placed back intra-abdominally and the abdominal wall was repaired. Afterwards, the rats were held inside the incubator for 30 minutes to recover within controlled surroundings.

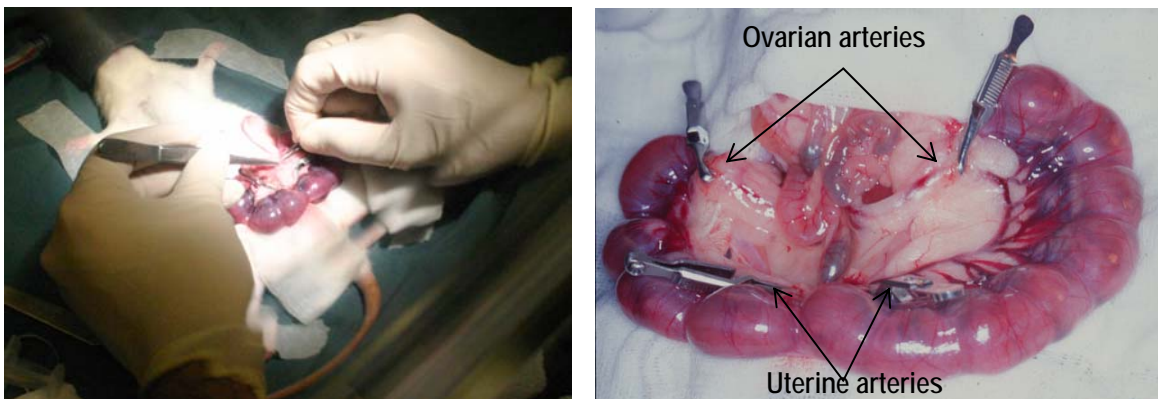


Figure 9: The fetal asphyxia procedure. The uterine horns were exposed using a laparotomy and the ovarian and the uterine arteries were clamped for 30 minutes with removable clamps.

Severe perinatal asphyxia

At embryonic day 21 or 22 (E21/E22), 18 date-pregnant rats (11 with mFA, 7 without mFA) were euthanized by decapitation and rapidly hysterectomized. The uterine horns containing the fetuses were detached. One uterine horn was placed in a water bath, precisely calibrated at 37°C, for exactly 18 minutes (counting from cutting off the blood circulation of the uterus to the moment the pups were taken from the water bath) [Fig 10]. After 18 minutes, the uterine horn was incised quickly and the pups were removed, cleaned with medical swipes and stimulated manually to breathe to aid recovery within the closed pediatric incubator (37°C, 60-80% humidity, room air). They were then left to recover for approximately 60 minutes in the same incubator. The umbilical cords were ligated and cut to separate the pups from their placentas. It is important to note that increasing the length of asphyxia to more than 20 minutes, leads to a mortality of 100%. The fetuses of the other horn were immediately delivered by opening the uterus and stimulating the pups as described above.

No more than two male pups per litter per condition were examined to prevent litter effects. They were randomly cross-fostered to surrogate dams, which have given birth normally the same day. Each surrogate mother received 10-13 pups. Body weight of the pups was measured at P0 and P8 or P15, respectively.

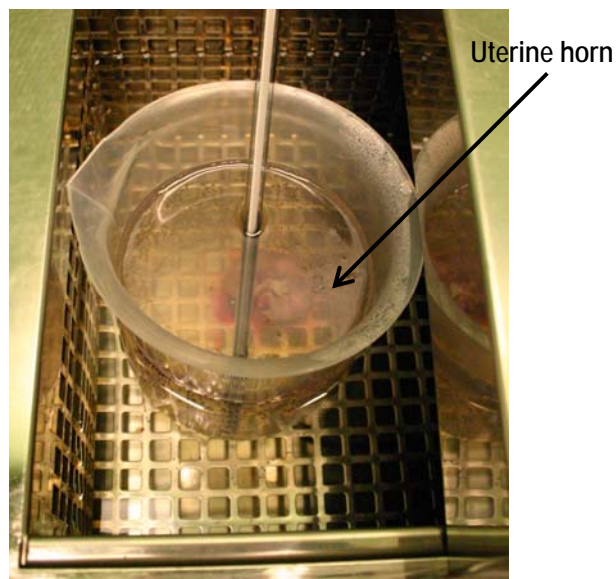


Figure 10: The severe perinatal asphyxia procedure. The uterine horns were detached from the mother and submerged in a water bath for 18 minutes.

2.2.2 Morphological analysis

Perfusions and tissue preparation

On the assigned days, postnatal day 8 (P8) and postnatal day 15 (P15), the pups were anesthetized with sodium pentobarbital (180mg/kg;i.p.;Nembutal). They were perfused intracardially (30/74 RPM), first by a flush of tyrode solution (30s), followed by fixative (10.30 min)

containing 4% paraformaldehyde and 0,2% picric acid in 0,2 M phosphate buffer (pH 7,2; RT). After the perfusions, the brains were removed from the skull and postfixed for 24h in 4% paraformaldehyde at 4°C. The brain tissue was cryoprotected by immersion in 10% sucrose/0,1M phosphate buffer overnight, followed by immersion in 20% sucrose/0,1M phosphate buffer for 48h both at 4°C. Afterwards, the brains were quickly frozen and stored at -80°C until further processing. The right hemispheres were cut into series of 30- μ m-thick sections on a cryostat (Leica CM 3050; Leica, Nussloch, Germany), while the left hemispheres were cut into series of 16- μ m-thick sections.

Terminal deoxynucleotidyl transferase-mediated dUTP-biotin nick-end labeling staining

To identify cell death a terminal deoxynucleotidyl transferase-mediated dUTP-biotin nick end-labeling (TUNEL) staining was performed. The TUNEL technique is used for the characterization of DNA fragmentation, particularly for the detection of single-strand breaks. It is based on the specific binding of terminal deoxynucleotidyl transferase (TdT) to the 3'-OH ends of fragmented DNA. TdT is used to incorporate biotinylated deoxyuridine at sites of nuclear DNA breaks.

Every eighth section was mounted on gelatinized glass slides and used for TUNEL staining as described before by Van de Berg *et al.* [14]. Briefly, sections were washed with TBS. Then, they were permeabilized for 10 min using methacarn (methanol:chloroform:acetic acid, 66:33:1) and rinsed in TBS (3 times 10 min). Subsequently, DNA fragments were labeled with the reaction mixture in a humidified box at 37°C for 1.5h. This reaction mixture consisted of 0.1 μ l TdT (400U/ μ l); 1 μ l cobalt chloride (2.5 mM); 2 μ l TdT reaction buffer; 0.4 μ l biotin-dUTP (2 nM); 6.5 μ l MilliQ (Roche Diagnostics Nederland B.V., Almere, Netherlands). During incubation, sections were covered with 10 μ l of the reaction mixture and coverslipped with parafilm. The reaction was stopped by placing the slides in 4x standard saline citrate (SSC) buffer (300 mM sodium chloride, 30mM sodium nitrate, pH 7.5) for 5 min at RT, followed by two 5-minute washing steps in TBS. Next, streptavidin-Alexa 594 diluted in TBS containing 0.3% Triton X-100 (TBS-T) (1:2000 dilution; for 60 min at RT, Sigma, The Netherlands) was used to visualize nuclei labeled with biotinylated dUTP. After washing in TBS, sections were counterstained with Hoechst 33342 in TBS (1:500 dilution; 30 min at RT; Sigma, The Netherlands). The procedure was finished by washing with TBS for 10 min and enclosure with TBS:glycerol (1:3).

Quantitative analysis of TUNEL-stained cells

TUNEL-positive cells were counted in the striata of left hemispheres of 4 rat pups of each group (CCD, sPA, mFA en mFA+sPA), sacrificed at P8. For each brain, 12 stained sections between Bregma 1.60mm and Bregma -1.80mm were analyzed. To detect the presence of positive cells, all slices were examined at a magnification 40x with an Olympus AX-70 microscope (using the counting method described by Van de Berg *et al.* [14]). Delineation of the striatum occurred using corpus callosum and lateral ventricle as landmarks, like depicted in figure 7. All TUNEL-stained

cells were easily identified by their intense and selective red color and they were counted regardless morphology. An estimation of the total number of positive cells in each rat was made by multiplying the sum of TUNEL-stained cells in all slides by the sampling interval (equal to eight). Furthermore, every TUNEL-positive cell was with the Hoechst 33342 staining to seen whether that particular cell was highly pyknotic and whether the nucleus was fragmented. All results were expressed in mean total number of TUNEL-positive cells per striatum and the number of TUNEL-positive cells per mm³.

Stereological analysis: volume estimates

For stereological analysis the right hemispheres of 4 rat pups of each group (CCD, sPA, mFA en mFA+sPA), sacrificed at P8, were used. The right hemispheres were entirely cut to serial, 30µm-thick coronal sections. Sections were mounted on gelatinized glass slides, yielding 8–10 sections per animal. Sections were dried, defatted with a Triton-X100 solution and stained with cresyl violet for the detection of Nissl body in the cytoplasm of neurons (0.01%, 11 min). Slides were coverslipped with DePeX.

Estimates of the volumes of the striatum were calculated according to the Cavalieri's principle [55], like earlier described in section 2.1.2. Briefly, profile areas of the sections through the region of interest were measured by tracing the boundaries of that region on video images displayed on a computer. The volume was then calculated by multiplying the sum of the profile areas of all sections with the distance between the sections. The striatum were delineated according to the lines drawn in figure 7. Tracing was carried out with a stereology workstation and StereoInvestigator software (MicroBrightField, Williston, VT).

Statistical analysis

All data are presented as means + SEM. A two-way ANOVA test (mFA x sPA), followed by a Bonferroni post hoc test, was applied to analyze the effect of mFA, sPA, mFA+sPA on mortality, body weight, number of TUNEL-positive cells and striatal volume. Changes in birth weight between the pups that underwent mFA and the pups that did not, were tested by a Student's *t*-test. Differences were considered to be significant if $P < 0.05$. All calculations were done using the Statistical Package for the Social Sciences (SPSS 12.0 software).

3. Results

3.1 Part I: Fetal Asphyxia

3.1.1 Presynaptic bouton densities

To investigate if the short-term memory deficit, seen in the behavioral testing of the 19-month-old asphyctic rats (previous study), are related to alterations in presynaptic bouton densities, synaptophysin immunoreactivity was determined in the prefrontal cortex and striatum.

Fig 11 shows an example of the immunostaining in the striatum of a sFA animal. The synaptophysin immunoreactivity was restricted to small punctae, which were interpreted as representing presynaptic boutons. There were no apparent differences in the morphological appearance of the punctae between the two groups of animals. Fig 12A shows the results of the presynaptic bouton densities in the different layers of the frontal cortex. Fig 12B shows the results of the presynaptic bouton densities in the different regions of the striatum. For the prefrontal cortex, the mean presynaptic bouton densities were higher in the sFA group compared to the sham, although no significant differences were found. For the striatum, in contrast, significant results were found in all 4 regions. Severe FA animals showed lower mean presynaptic bouton densities in the dorsal (-15.3%; $P=0.015$), the lateral (-18.3%; $P=0.014$), the medial (-14.4%; $P=0.025$) and the ventral part (-20.0%; $P=0.024$), as well as the pooled data of the total striatum (-17.1%; $P=0.017$). Taken together, these data indicate that there is a decrease in presynaptic bouton density in the striatum of animals who suffered from sFA.

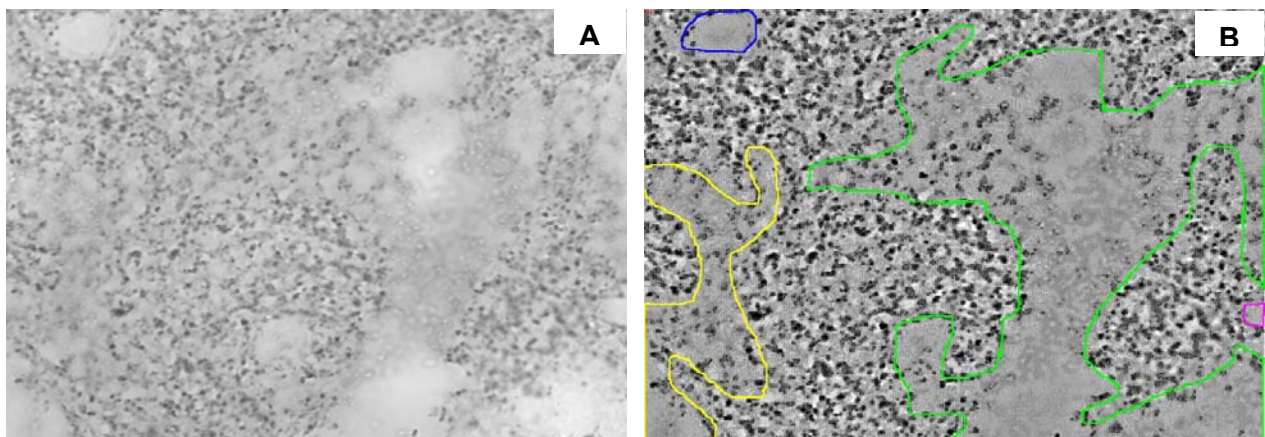


Figure 11: Example of an image of a synaptophysin-stained area in the striatum of a 19-month old fetal asphyctic animal as obtained by the image analysis system. (A) Unedited picture, showing the gray levels of the synaptophysin staining. (B) Edited image, showing the modified gray scale punctae. Blood vessels, neuronal cell bodies, artifacts and areas not in focus were excluded from the analysis (colored delineated areas).

3.1.2 *Volume estimates*

To study and compare the volumes of the regions of interest between the sFA and the sham animals, volume estimates were calculated. Fig 12C and 12D show the volume estimates of the prefrontal cortex and the striatum. Analyses of the volume estimates of the layers of the prefrontal cortex indicate a rise in mean volumes in sFA animals as compared to sham animals. The extent of those increases in the different cortical layers, however, was not uniform. The 1st (+21.0%; $P=0.0347$) and the 6th layer (+14.2%; $P=0.0064$) of the sFA animals showed a significant increase in comparison to the sham animals. There was a trend towards a significant increase following sFA in the volumes of the 2nd (+8.7%; $P=0.0545$) and 4th layer (+18.8%; $P=0.0681$), as well as in the pooled value of the total prefrontal cortex (+16.2%; $P=0.0922$). The 3rd and the 4th layer showed a similar pattern, though no significant differences could be found. Analyses of the striatal volume could not detect a significant difference between the sFA and the sham group. Altogether, these data point towards an increase in the volume of the prefrontal cortex, but not of the striatum.

3.1.3 *Number of synapses*

From the data described above it is not possible to calculate the exact total number of synapses, because the size, shape and orientation are unknown. An evaluation of the alterations in the number of synapses between the groups was made by multiplying the density of the presynaptic boutons by the volume estimates, without taking into account the exact dimensions. Fig 12E and 12F show the results of the analyses of the mean number of synapses of both groups. In case of the prefrontal cortex, higher numbers of synapses were found in all of the investigated layers after sFA. None of those changes were significant, except for the 5th layer which showed a trend towards significance (+75.3%; $P=0.0921$). Analysis of the striatum, on the contrary, illustrated a significant decrease (-37.6%; $P=0.0155$) in the number of synapses following sFA. Overall, these data show a decrease in synapses in the striatum and a trend towards an increase in the 5th layer of the prefrontal cortex.

Presynaptic bouton density

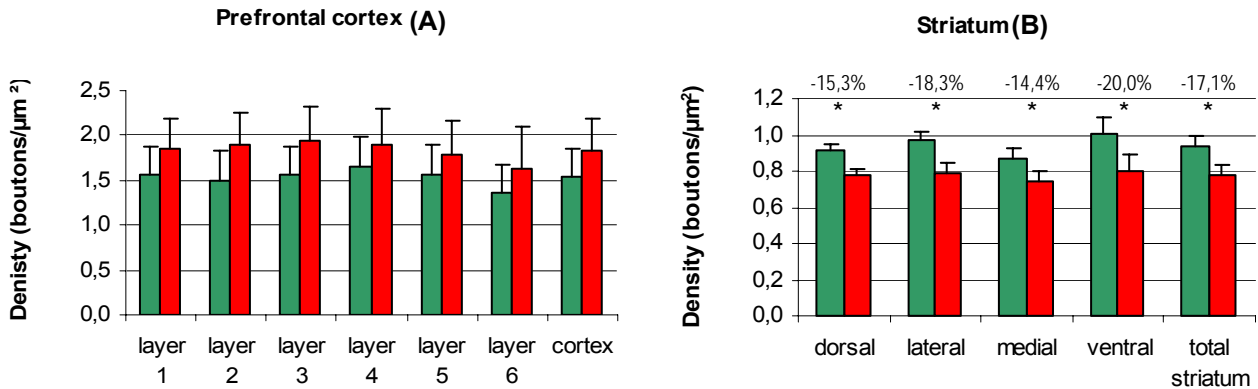


Figure 12: Presynaptic bouton densities, volume estimates and number of synapses investigated in the prefrontal cortex (A, C and E) and the striatum (B, D, and F) of sham-operated rats (■ ; n=5) and severe fetal asphyctic (sFA) rats (■ ; n=5) at the age of 19 months. Data are expressed as mean + SEM. (A) There was no significant difference in presynaptic bouton density between the sFA group and the sham group. (B) There was a significant difference in presynaptic bouton densities of all four regions of the striatum and the total striatum. (C) A significant increase in volume of the 1st and 6th layer was found in the sFA group compared to the sham group. There was a tendency towards significance in layer 2, layer 4 and the total cortex. (D) No significant alterations in striatal volume were found between the sFA and sham rats. (E) There was a tendency towards significance of the number of synapses in layer 5. No significant differences could be found in the other layers. (F) A decrease in the number of synapses was found in the sFA group compared to the sham group. (* $P < 0.05$ and # $0.05 < P < 0.1$)

3.2 Part II: Hypoxic-ischemic preconditioning

3.2.1 Neonatal mortality

A frequent and a severe complication of birth asphyxia is death. To assess if preconditioning had an effect on this aspect, mortality rates were calculated. Table 4 shows the results of the neonatal mortality rates, expressed as mean mortality per litter. In our model, 55% of the animals per litter died after a sPA insult of 18 minutes, while none of the mFA or CCD animals died. When the pups had a mild prenatal hypoxic exposure before being exposed to a severe perinatal insult, fewer animals per litter died (39%). This difference in mean mortality rate per litter between the sPA and the mFA+sPA did not reach statistical significance ($P=0.187$).

Table 4: Mortality rates, expressed as mean per litter, of the different experimental groups at postnatal day 0 (Mean \pm SEM).

Groups	Mortality
Control (CCD)	0%
mFA	0%
sPA	55.22% \pm 0,20
mFA+sPA	38.99% \pm 0,36

(CCD: control caesarian delivery; sPA: severe perinatal asphyxia; mFA: mild fetal asphyxia)

A few pups died in the period between P0 and P15 as well. An overview of the survival rates is given in figure 13. All of the CCD pups and 90% of the mFA pups survived the end of the experiments (until day 15). In contrast, only 26% of the sPA pups survived, while still 44% of the mFA+sPA pups did. Furthermore, it is important to note that none of the fetuses died in the period between the mFA insult at E17 and birth. In summary, sPA has an immense effect on the survival of rat pups, which seemed to be improved by a preceding, less damaging event.

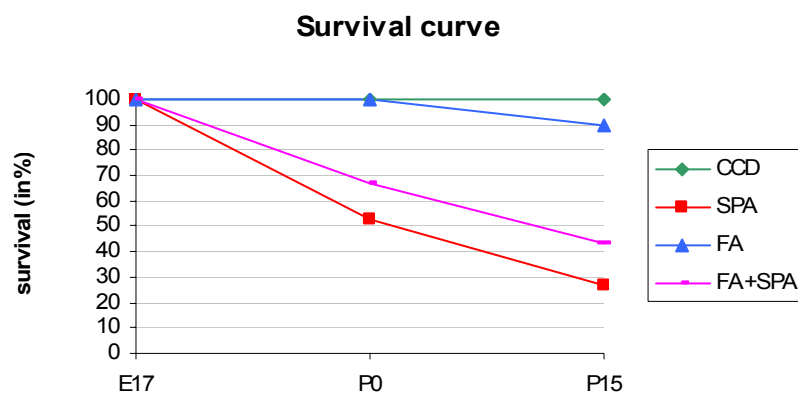


Figure 13: Survival curve of the different experimental groups. None of the CCD pups and only 10% of the mFA pups died during the experiments. The survival rate was higher in the mFA+sPA group compared to the sPA group at both postnatal day 0 (P0) and postnatal day 15 (P15). This difference did, however, not reach statistical significance.

3.2.2 Birth weight

To see if the insults had an effect on the fetus, birth weights were measured at P0 after recovery. As depicted in figure 14 the mean body weight at P0 of the pups which underwent mFA (mFA and mFA+sPA pups) was lower than the mean body weight of the pups which did not undergo the insult (CCD and sPA pups). This decrease in birth weight (-7.3%) showed a tendency towards significance ($P=0.054$). The sPA insult did not cause any changes in the body weight at P0 (data not shown).

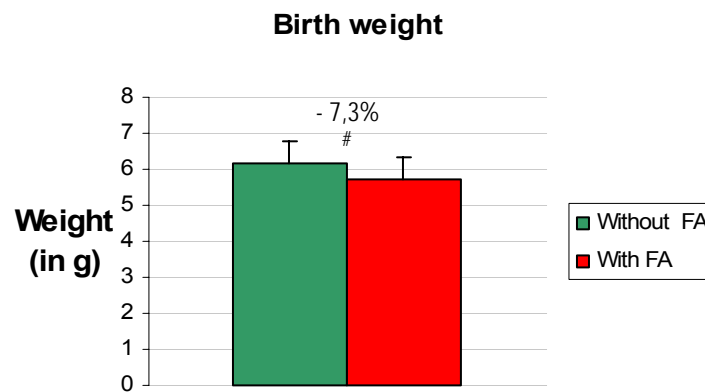


Figure 14: The body weight of the pups at postnatal day 0. The pups which underwent a mFA (mFA and mFA+sPA) insult have a smaller body weight than the pups which did not undergo a mFA insult (CCD and sPA). This decrease in body weight is not significant, but has a tendency towards significance. (# $0.05 < P < 0.1$) (mFA = mild fetal asphyxia; sPA = severe perinatal asphyxia)

2.2.3 Body weight

Body weights were also measured throughout the course of the study at P8 and P15. Mean body weights at the different time points are given in figure 15. The tendency towards a decrease in birth weight following fetal asphyxia [Fig 15], seen at P0, completely disappeared at P8. There was no difference anymore between the mFA/mFA+sPA and the CCD animals. At that time point, however, the sPA pups underwent growth retardation in comparison to the other groups. Their mean body weight was lower than the mean weight of the other groups. Furthermore, their mean weight was 5.6% less than the mean weight of the pups which underwent mFA before sPA ($P=0.049$). The mean body weights of the mFA and mFA+sPA groups at P8 did not differ from the control group. At P15, the mean body weights of the sPA pups were still lower in comparison to the other groups, although no significant difference could be found.

To sum up, mFA has an early effect on the birth weight of pups, which disappears a week after birth, whereas sPA causes a growth retardation at P8 and P15. This growth retardation is overcome by a preceding mFA incident.

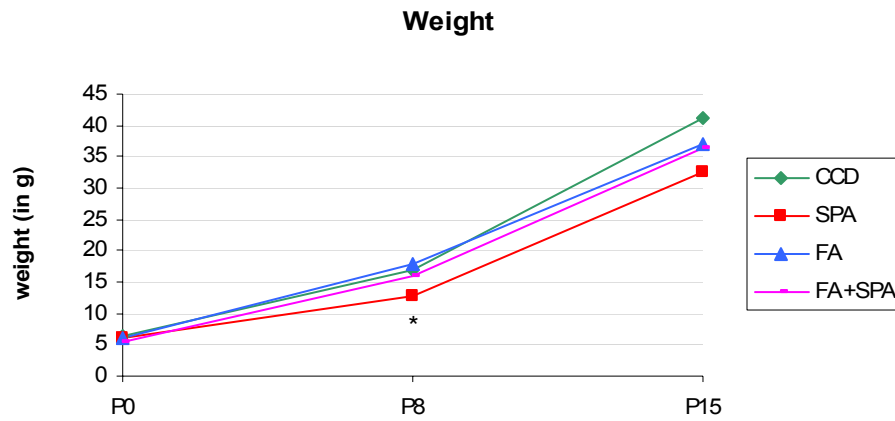


Figure 15: The body weights of the pups at the different time points (P0, P8 and P15) of the study. At P0, there is a trend towards a significant effect of fetal asphyxia on birth weight. At P8, the mean body weight of the sPA group was lower than the mean weight of the other groups, meaning that the sPA pups undergo growth retardation ($P=0.049$), while there is no difference in body weight between the other groups. At P15, the weight of the PA pups is still less than the other groups, but the difference does not reach significance anymore. (* < 0.05)

3.2.4 General observations

During the period immediately after the insult, the effect of sPA was evident on breathing, motility and color of the skin. sPA and mFA+sPA pups recovered very slowly after stimulation. They showed gasping and almost no movement. Their skin color was very pale. Furthermore, feces were found in almost all the placentas of the sPA and mFA+sPA pups, pointing towards a hypoxic bowl. Similar effects are observed in human asphyctic neonates. CCD and mFA pups, in contrast, started regular breathing immediately after birth and showed a normal, pink-colored skin and normal motility.

No gross morphological changes could be seen in the brain of asphyctic pups compared to the CCD pups 8 days after delivery. Typical apoptotic morphological changes like condensation, shrinkage and fragmentation were found in all four groups and were visible with both the TUNEL and the Hoechst staining [Fig. 16]. TUNEL-stained cells were mainly found in the surrounding area of the lateral ventricle and the corpus callosum and in the dorsal part of the striatum. Mostly, they are together in clusters, showing a patchy pattern.

3.2.5 TUNEL

One of the most important features of asphyctic damage is delayed apoptotic cell death. To evaluate the effect of preconditioning on cell death in the different experimental groups, TUNEL-labeled sections were analyzed in the striata of 8-day-old rat pups. Figure 17A summarizes the results of the quantitative analysis of the TUNEL stained cells.

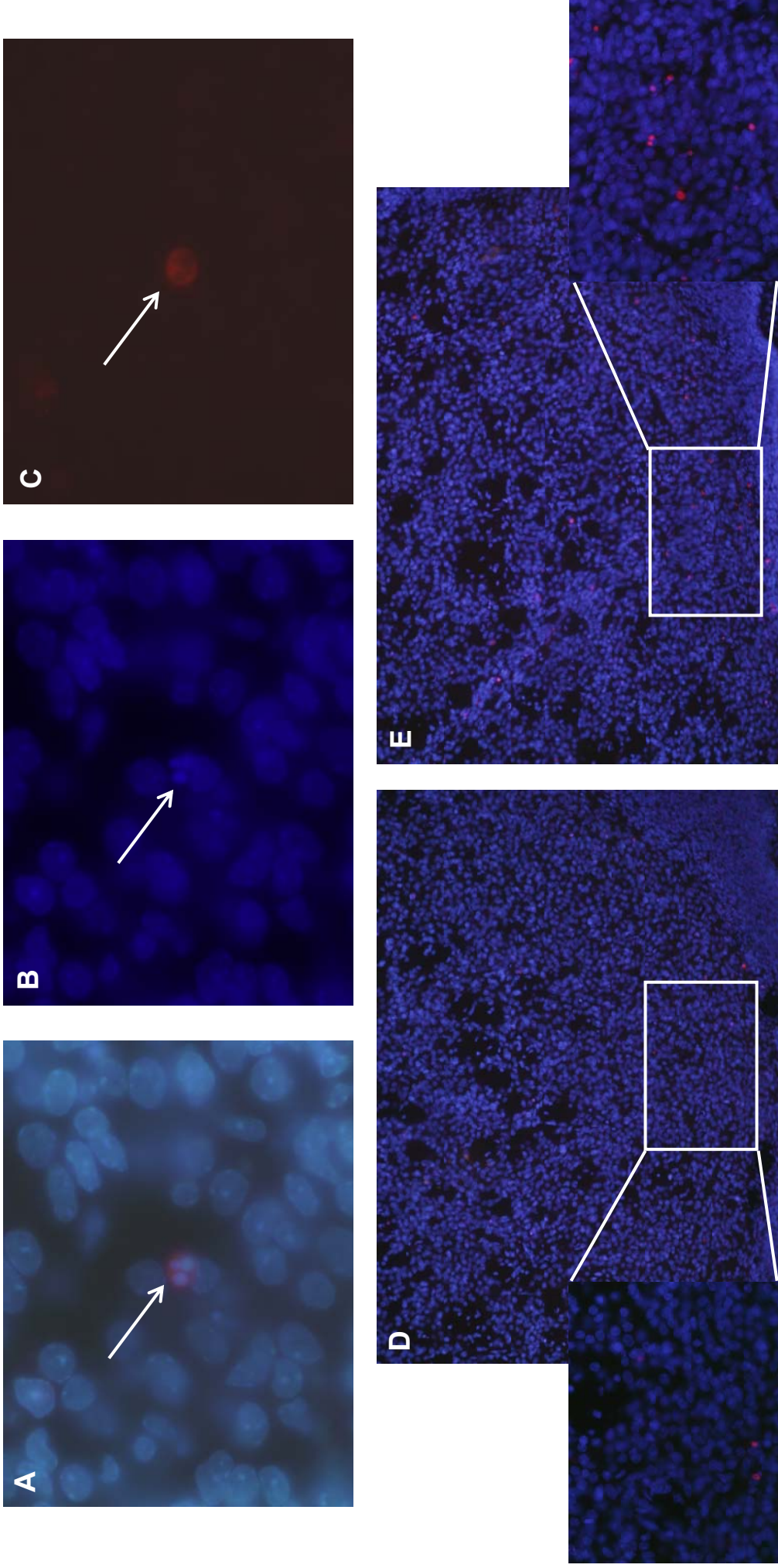


Figure 16: Photographs of normal and apoptotic cells in the rat striatum 8 days after a severe perinatal insult. (A) Overview showing both the TUNEL staining and Hoechst contrasting at magnification 100x. Fragmented nuclei are visible (Arrow). (B) Section showing the Hoechst contrasting at magnification 100x, also showing the fragmented nuclei (Arrow). (C) Section only showing the TUNEL staining at magnification 100x. One apoptotic cell is detectable, showing the fragmented nuclei (in red) (Arrow). (D) Almost no apoptotic cells (in red) are visible in the striatum of mFA+sPA animals (magnification 20x). (E) A lot of apoptotic cells (in red) can be detected in the striatum of sPA animals, especially in the vicinity of the lateral ventricle (see circle).

Two-way ANOVA analysis revealed a slight, but significant increase in the total number of apoptotic cells due to a mFA insult ($P=0,03$). Both the mFA and the mFA+sPA group showed higher total numbers of apoptotic cells than the CCD group, although post-hoc Bonferroni testing could not detect any significant differences between those groups. For that reason it seems that a mFA insult does not cause that much apoptotic cell death.

Severe PA also significantly increased the total number of apoptotic cells (two-way ANOVA; $P=0,01$). This difference could be almost completely attributed to the sPA group, and not the mFA+sPA (post-hoc Bonferroni, CCD versus sPA: $P=0,01$; CCD versus mFA+sPA: $P=0,678$).

As expected, brains subjected to mFA before undergoing sPA demonstrated a significant reduction (-46,4%) in apoptotic cells compared to the brains only subjected to sPA, as demonstrated by post-hoc Bonferroni analysis ($P<0,001$). This difference between both groups is clearly depicted in figure 16 D and E. Consequently, it appears that the preconditioning effect did almost totally prevent the damaging effect of sPA.

3.2.6 Volume estimates

To see if any of the insults caused alterations in the size of the striatum, volume estimates were obtained in the same rat brains as used for TUNEL analysis. The results are depicted in figure 17B. The mean volume of the CCD group seems slightly higher compared to the mean volume of the different groups subjected to an insult. Two-way ANOVA analysis, however, revealed no significant decrease due to mFA, sPA or the interaction of both. Post-hoc Bonferroni analysis could not detect any alteration between the groups either.

Taking into account both the data of the TUNEL-positive cell counting and the volume measurements, estimations of the density of apoptotic cells could be calculated. The results of the number of TUNEL positive cells per mm^3 are given in figure 17C. Mild FA caused a small increase in the mean density of apoptotic cells (two-way ANOVA; $P=0,02$). However, post-hoc Bonferroni analysis could not find any significant differences between both mFA groups and the CCD group. Two-way ANOVA analysis also revealed a significant increase in the mean density of apoptotic cells due to sPA (in sPA and mFA+sPA groups) ($P<0,001$), which could be almost entirely ascribed to the sPA group (post-hoc Bonferroni; CCD versus sPA: $P<0,001$; CCD versus mFA+sPA: 0,558). Moreover, post-hoc Bonferroni testing demonstrated that the mean density of apoptotic cells in the mFA+sPA group was significantly lower than in the sPA group ($P<0,001$).

Together the results of the total number and density of apoptotic cells indicate that mFA seems to provide strong protection against apoptotic cell death caused by sPA.

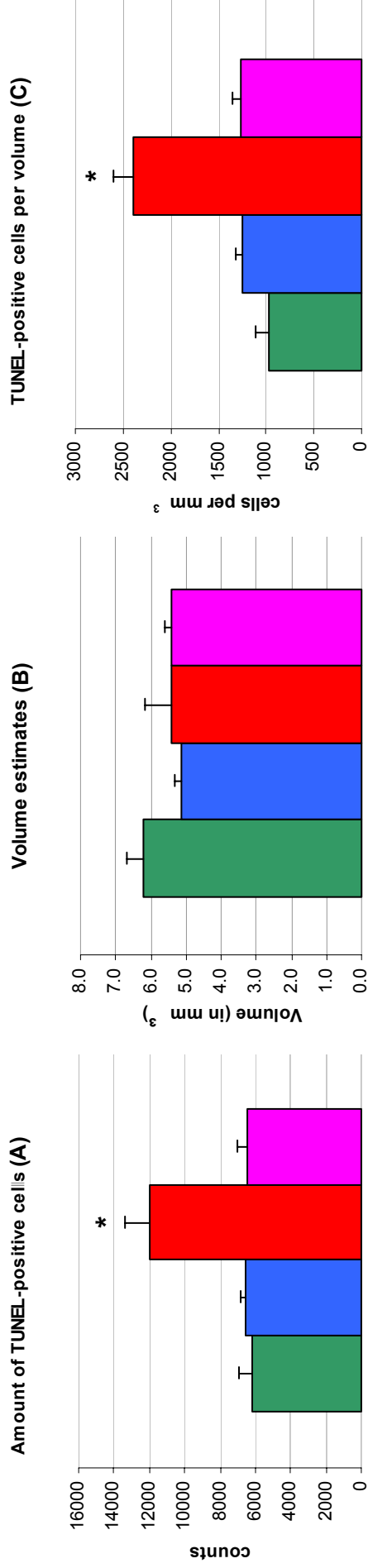


Figure 17: Quantitative analysis of the TUNEL-positive cells and the volume of the striatum of 8-day-olds rat pups of the different experimental groups (Control Caesarean Delivery (CCD), $n=4$; mild Fetal Asphyxia (mFA), $n=4$; severe Perinatal Asphyxia (sPA), $n=4$ and mild Fetal Asphyxia+severe Perinatal Asphyxia, $n=4$). Data are expressed as mean \pm SEM. (A) There is a significant increase in TUNEL-positive cells in the sPA group compared to the other groups ($P<0.001$). Hypoxic-ischemic preconditioning protected against delayed programmed cell death in the mFA+sPA group. The mean number of positive cells was very low and was significantly different from the sPA group ($P<0.001$). It did however not differ from the mFA and CCD group. (B) Although the mean volume of the striatum seems higher in the CCD group, no significant differences could be found between the any of the groups. (C) The number of TUNEL-positive cells per mm³ was significantly higher in the sPA group than in the mFA+sPA group, pointing towards a protecting effect of fetal asphyxia. The mean number of positive cells per mm² seems slightly lower in the CCD group compared to the mFA and mFA+sPA, although this difference was not significant.

4. Discussion

4.1 The long-term effect of severe fetal asphyxia

The present study shows that a severe fetal asphyctic insult during pregnancy, a critical period for the development of the brain, can have long-term effects on synaptic organization. Nineteen-month old sFA rats showed a tendency towards an increase in presynaptic bouton numbers in the fifth layer of the prefrontal cortex, while a clear decrease was found in the striatum. There the presynaptic bouton density and numbers were significant lower in the sFA group compared to the sham-operated animals. Furthermore, asphyctic rats had a larger prefrontal cortex.

Alterations in presynaptic bouton densities have been reported many times before, for example in relation to aging or neurodegenerative diseases, but also as a result of hypoxic or ischemic damage to the brain [25]. Parts of our data are in line with those previous reports in the literature, while others are conflicting. With respect to long-term hypoxic damage, others observed increases in presynaptic bouton density. For example, Stroemer et al. have shown an increase in the cortex following cerebral ischemia [26]. Accordingly, Van de Berg et al. revealed similar increases in both the striatum and the parietal cortex after severe perinatal asphyxia [14]. Long-term decreases in presynaptic bouton density in relation to FA have never been published before. An explanation for the difference with the current literature could be that a distinct animal model is used. The studies described above used models for perinatal asphyxia, while in this study a model for fetal asphyxia is applied. The most important difference between both models is the timing of the insult. Consequently, timing might play an important role in determining the injury pattern following asphyxia in infants, probably due to different developmental stages of the immature brain.

There are several possible hypotheses that might explain the decrease in presynaptic bouton density and number in the striata of sFA rats. The decrease may be due to an incomplete recovery of the synapse loss that occurs in the first minutes and hours after the hypoxic-ischemic insult. Several studies demonstrated that decline in both pre-and postsynaptic density immediately after the insult. For example, transient global perinatal ischemia causes a marked decrease in postsynaptic density the hippocampus of chickens and fetal hypoxia cause a similar decrease in presynaptic numbers in 1 day old rats [28, 29]. There are also studies demonstrating recovery after hypoxic-ischemic injury. Accordingly, Engert et al. found an increase in synapses starting 24h after the hypoxic exposure in cell cultures compared to the number immediately after the exposure [62]. However, none of the studies mentioned above investigated whether the repair process was only partial or complete. Studies that examined long-term effects of severe FA or PA, showed that there is still synapse damage a couple of weeks after the exposure. Yang et al. showed, by looking at SynGAP, a protein playing an essential role in synaptic plasticity, that there was still a synapse

defect 45 days after perinatal hypoxia [63]. Accordingly, Ramirez et al. detected altered phospholipids patterns 30 days after hypoxia-ischemia, pointing to the fact that there was still a reduction in synaptogenesis at that time point [64]. Although the last two reports are in line with the explanation of an incomplete recovery, the results of behavioral testing of the sFA animals, executed in a previous study within our group, do not demonstrate any early changes. The sFA animals performed normally during MWM and OF testing until the age of 19 months (see appendix).

Therefore, an alternative explanation is that the decrease observed in the striata of our sFA animals may represent an acceleration of the aging process. Aging leads to synapse loss in a number of brain regions, like the striatum, the prefrontal cortex and the hippocampus [25, 65]. Wong et al. reported a reduction in presynaptic bouton density in the cortex of older rats compared to their younger counterparts [25]. Similar results have come forward from human studies, showing a loss in synaptic input in the frontal cortex of older individuals [24]. Arguments in favor of this explanation are the results of the behavioral testing of the investigate asphyctic animals (see appendix). MWM and OF tests showed no differences at 1.5, 6 or 12 months. At 19 months, however, sFA rats swam longer distances to find the platform compared to sham controls, indicating an impaired short-term memory. In the OF test, those 19-month old sFA animals showed shorter distances moved and longer time spent in the corners, both pointing towards anxious behavior. These results are comparable to the defects seen in aging rats. Furthermore, comparable memory impairments have been found in other asphyxia models. Severe perinatal asphyxia causes an exaggerated age-related long-term memory deficit [15]. Altogether, sFA may accelerate aging in cognitive and spatial learning by a reduction in synaptic connectivity.

Regarding both explanations, several factors might contribute to the reduction in synaptic density and number in the striatum of sFA animals. First, it may be due to death of neurons as a result of e.g. programmed cell death or oxidative stress [25]. Second, it may be caused by neuronal changes, like degeneration of dendritic structures or retraction of axonal processes intruding on the striatal neurons [66]. Both dendrite regression and lower dendritical spine densities have been related to synapse loss in aging [67]. This awaits further research though.

Another important finding of this study is the regional difference in presynaptic density and numbers. While there is a presynaptic depletion in the striatum, the fifth layer of the prefrontal cortex shows a tendency towards an increase in presynaptic bouton numbers. This difference between both areas can also be clarified by a few potential mechanisms. A first potential mechanism is that the aging process shows a spatiotemporal phase shift. Aging sometimes begins with neuritic growth and enhanced synapse formation in the early stages, followed by regression of dendrites in older animals [68]. In our animals, the aging process may have been started in the

striatum before the age of 19 months, showing a decrease in synapses, while the aging may only just have begun in the prefrontal cortex, showing a tendency towards enhanced synapse formation. The second potential mechanism is a compensatory mechanism. The observed increase in presynaptic bouton density and numbers in the prefrontal cortex may be an attempt to compensate for the loss of synapses in the striatum and maybe also in other regions of the sFA brains by allowing more neuronal communication. Similar compensatory mechanisms between two different areas are already demonstrated in neurodegenerative diseases, like Alzheimer's disease [69]. The increase in volume of some of the cortical laminae, observed in our sFA animals could be part of the same compensation effort trying to recompense for the synapse loss in the striatum. Moreover, the sFA brains could also try to adjust for a possible loss in neuron numbers by the formation of new synaptic connections.

In conclusion, severe fetal asphyxia leads to a long-term decrease in presynaptic bouton density and number within the striatum, while it leads to a tendency towards an increase in presynaptic numbers in the fifth layer of the prefrontal cortex. This striatal decrease is may be caused by an acceleration of the aging process, mediated by changes in dendrite number, axonal alterations or neuronal loss. The difference between the two regions could be explained by a compensatory mechanism or a spatiotemporal phase shift. Whether this holds true awaits further research. For example, looking at neuron numbers in both the prefrontal cortex and striatum, could exclude the possibility that the loss of synapses is due to a reduction in neuron numbers. To shed light on the fact that synapse recovery after sFA may be incomplete, synaptophysin immunoreactivity has to be examined at different time points between the insult and the loss seen at 19 months.

4.2 Mild fetal asphyxia and its role in preconditioning

Birth asphyxia is a major cause of neonatal mortality and of subsequent lifelong neurological disabilities among those infants who survive it. Although our understanding is increased considerably the last years, there is still no pharmacological treatment available. Revealing the mechanisms behind hypoxic-ischemic preconditioning and tolerance could therefore be an important step towards an effective therapy. The objective of this pilot study was to determine if mFA protects against subsequent sPA. To achieve this goal, the number of apoptotic cells was analyzed in the striata of 8-day-old rats after 18 minutes of sPA, with or without a preceding 30-minute-mFA insult, using a TUNEL staining. The TUNEL method allows detection of nuclear DNA fragmentation in cells. Although fragmentation is a pattern typical for apoptosis, it can also occur, to a lesser extent, in necrotic cells. As a consequence, TUNEL can occasionally also stain necrotic cells. Because each stained cell was analyzed for apoptotic traits like nuclear fragmentation and a pyknotic nucleus with a Hoechst staining, we assume that the majority of counted cells were apoptotic.

In the CCD group, only a few apoptotic cells were found. This kind of apoptosis probably represents naturally occurring developmental cell death. The mFA group showed slightly higher levels of apoptotic cells compared to the CCD group, although this difference did not reach statistical significance. The sPA group, in contrast, showed a substantial increase in TUNEL-positive cells. Pups that underwent mFA before being subjected to sPA had significantly less apoptotic cells than pups that did not undergo mFA, suggesting a protective effect. Their number of apoptotic cells were similar to that of the CCD and the mFA group. Another important finding of this study is that the mortality rate seemed to be lower in the mFA+sPA group than in the sPA group. This difference in mortality did, however, not reach statistical significance, most likely due to a low power. Increasing the number of animals in each group in the next study, may possibly reveal significant differences. Since the mFA insult was global, this protection may include protective effects of many organs and systems, such as the heart and the arteriovenous system, to accomplish the decreased mortality rate. Taken together, these differences between the mFA+sPA and the sPA group indicate that mFA seems to protect against harmful effects like delayed apoptotic cell death and increased mortality, normally caused by sPA.

It is important to note that this second study uses a mild form of fetal asphyxia (30 min) in stead of the severe form (75 min) used in the first study of this project. While sFA causes substantial long-term consequences (e.g. changes in synaptic organization), it seems that mFA has a neuroprotective effect, without causing apoptotic cell damage.

Though this study is the first to look at hypoxic-ischemic preconditioning and tolerance in a global asphyxia model, current findings are consistent with cell protection by hypoxic-ischemic preconditioning against focal asphyctic injury (=stroke model). Cantagrel et al. found that exposure of the pregnant dam to a hypoxic gas mixture (8% O₂/92% N₂) causes a reduction in the number of apoptotic cells in the striatum, hippocampus and cortex 24h and 48h after right carotid ligation at postnatal day 7 (Rice-Vannucci model) [70]. In the same rat model, Zhao et al. demonstrated that newborns with prenatal asphyxia showed lower mortality rates, less brain tissue damage, less neuronal loss and fewer caspase-3 positive cells [71]. Accordingly, Cai et al. demonstrated that another prenatal hypoxia-ischemia insult, achieved by clamping the ovarian and uterine arteries for 30 min, also reduces the brain infarct size and neuronal injury induced by the Rice-Vannucci model [41]. Of note, similar decreases in apoptotic cells after preconditioning have been observed in other organs like kidney and heart [72]. Asphyxia-induced preconditioning is not only detectable at the morphological level. It can be seen at behavioral level, as well. Rats exposed to a preconditioning hypoxic insult 24h before severe perinatal asphyxia significantly improved in terms of orientation and memory function, while no such improvement was seen in the rats not exposed to a preconditioning insult [48].

Though a number of different mechanisms and molecules have been linked with various types of preconditioning, the mechanisms underlying the delayed phase of preconditioning-induced neuroprotection are still unknown. Nevertheless, it has been suggested that three groups of molecules are involved in hypoxic-ischemic preconditioning: sensors, transducers and effectors [73][Fig 18]. Together, this set of molecules form a complex cascade that senses a triggering signal (e.g. hypoxia) and amplifies it into several effector functions, inducing a protective effect. HIF-1 has been suggested as at least one of the sensor molecules for prenatal hypoxia, because its subunit α is an oxygen-sensitive unit. Moreover, animals treated with compounds known to induce HIF-1, like cobalt, are protected against ischemic injury in the brain [74]. In addition, a hypoxic trigger increases HIF-1 α -transcriptional activity of target genes related to vasomotor control (NOS2), angiogenesis (VEGF), iron metabolism (EPO), cell proliferation (TGF β) and energy metabolism (GLUT-1), all processes important for neuroprotection, as reviewed by Ran et al. [51]. Another molecule that might function as a sensor is the NMDA receptor. In many models, hypoxic-ischemic preconditioning requires NMDA-receptor activation and NMDA receptor antagonists can block ischemia-induced preconditioning [75]. A preconditioning stimulus may for example affect the subunit composition of the receptor. NOS has been suggested as one of the transducers of neuroprotection induced by hypoxia-ischemia, because application of 1400W, an inhibitor for iNOS, before prenatal hypoxia abolished the protection against perinatal hypoxia. In addition, iNOS expression is upregulated 3h after the hypoxic prenatal stimulus [71]. Other studies demonstrated that the RAS-phosphorylation pathway of ERK may also be an important signal-transduction pathway for neuroprotection [76]. The effectors, contributing to preconditioning, may include many protective proteins like heat shock proteins and anti-apoptotic proteins, which are known to be

upregulated by a hypoxic-ischemic stressor or insult. The levels of Bcl-2, a pro-apoptotic molecule, are increased a few hours after the preconditioning insult, while the levels of Bim and other anti-apoptotic factors are decreased [77]. The transcription factor driving the induction of Bcl-2, CREB, is highly activated by phosphorylation as well [78]. Prenatal asphyxia may therefore change the balance between pro- and anti-apoptotic proteins.

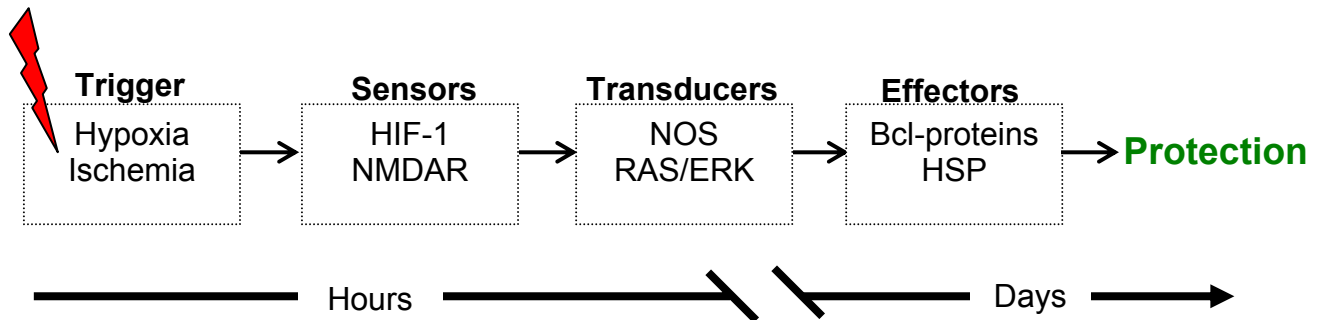


Figure 18: Schematic overview of some of the mechanisms that may be involved in the delayed phase of hypoxic-ischemic preconditioning in the immature rat brain, according to the current literature. Three groups of molecules are important for hypoxia-ischemia-induced neuroprotection: sensors, transducers and effectors. Examples of sensors are hypoxia-inducible factor 1 (HIF-1) and the N-methyl-D-aspartate receptor (NMDAR), which play an important role during the first hours after hypoxia or ischemia. Examples of transducers are nitric oxide synthase (NOS) and the RAS/ ERK phosphorylation pathway. Their period of action ranges from a few hours to a few days after the preconditioning insult. Some of the potential effectors, responsible for the ultimate neuroprotecting effects are heat shock proteins (HSP) and bcl-proteins. (Adapted from Dirnagl et al, 2003)

An important remark to be made is that the neuroprotective effects induced by mFA in this study may be partly due to the anesthetics. Kersten et al. reported that isoflurane can mimic the protecting effects of preconditioning in the rat myocardium, while Kapinya et al showed that isoflurane induces prolonged protection against cerebral ischemia [79, 80]. Moreover, caesarian section per se induces specific neurobehavioral alterations with respect to for example response to stress, and the addition of a period of asphyxia worsens some of the behavioral changes produced by C-section alone [81]. Consequently, isoflurane and caesarian section can possibly influence the results of the apoptotic cell counts. For that reason, it is important to include vaginally-delivered controls and sham-operated controls in the next study.

In conclusion, animals exposed to a brief period of mFA seem to be protected against apoptotic damage in the striatum, following sPA 4 days later. This hypoxia-ischemia preconditioning is most likely the result of the delayed phase of neuroprotection, which requires new protein synthesis and gene expression. This anti-apoptotic effect probably involves several molecules, as described above, that are induced and regulated as part of a complex. To imply the role of these molecules in

prenatal hypoxia-induced tolerance, further experiments are required. One could for example look at expression levels of Bcl proteins, hsp proteins and NOS by Western blotting. Or use antagonists of HIF-1 or NMDAR to investigate if these molecules are involved in global hypoxic-ischemic preconditioning. Another important step could be to examine if the protection against apoptosis caused by mFA consequently leads to less neuronal loss, normally seen after sPA. Moreover, it is also important to look, not only at morphological changes, but also examine if hypoxic-ischemic preconditioning can protect against short and long-term behavioral alterations in our animal model, since sPA has substantial effects on for example motor function and memory in humans. Severe PA studies also showed changes in BDNF expression in sPA animals compared to controls. Therefore, it could also be interesting to see if the protecting effect of this neurotrophic growth factor may play a role in limiting the amount of cell death after hypoxic-ischemic preconditioning.

References

1. Low, J.A., *Relationship of fetal asphyxia to neuropathology and deficits in children*. Clin Invest Med, 1993. **16**(2): p. 133-40.
2. Pierrat, V., et al., *Prevalence, causes, and outcome at 2 years of age of newborn encephalopathy: population based study*. Arch Dis Child Fetal Neonatal Ed, 2005. **90**(3): p. F257-61.
3. Lawn, J.E., S. Cousens, and J. Zupan, *4 million neonatal deaths: when? Where? Why?* Lancet, 2005. **365**(9462): p. 891-900.
4. Low, J.A., *Determining the contribution of asphyxia to brain damage in the neonate*. J Obstet Gynaecol Res, 2004. **30**(4): p. 276-86.
5. Bracci, R., S. Perrone, and G. Buonocore, *The Timing of Neonatal Brain Damage*. Biol Neonate, 2006. **90**(3): p. 145-155.
6. Berger, R. and Y. Garnier, *Pathophysiology of perinatal brain damage*. Brain Res Brain Res Rev, 1999. **30**(2): p. 107-34.
7. Parer, J.T., *Effects of fetal asphyxia on brain cell structure and function: limits of tolerance*. Comp Biochem Physiol A Mol Integr Physiol, 1998. **119**(3): p. 711-6.
8. MacLennan, A., *A template for defining a causal relation between acute intrapartum events and cerebral palsy: international consensus statement*. Bmj, 1999. **319**(7216): p. 1054-9.
9. Boksa, P., A. Krishnamurthy, and W. Brooks, *Effects of a period of asphyxia during birth on spatial learning in the rat*. Pediatr Res, 1995. **37**(4 Pt 1): p. 489-96.
10. Younkin, D.P., *Hypoxic-ischemic brain injury of the newborn--statement of the problem and overview*. Brain Pathol, 1992. **2**(3): p. 209-10.
11. Weitzdoerfer, R., et al., *Long-term influence of perinatal asphyxia on the social behavior in aging rats*. Gerontology, 2004. **50**(4): p. 200-5.
12. Vannucci, R.C. and S.J. Vannucci, *Perinatal hypoxic-ischemic brain damage: evolution of an animal model*. Dev Neurosci, 2005. **27**(2-4): p. 81-6.
13. Loidl, C.F., et al., *Effects of hypothermia and gender on survival and behavior after perinatal asphyxia in rats*. Physiol Behav, 2000. **68**(3): p. 263-9.
14. Van de Berg, W.D., et al., *Perinatal asphyxia results in changes in presynaptic bouton number in striatum and cerebral cortex-a stereological and behavioral analysis*. J Chem Neuroanat, 2000. **20**(1): p. 71-82.
15. Dell'Anna, E., et al., *Delayed neuronal death following perinatal asphyxia in rat*. Exp Brain Res, 1997. **115**(1): p. 105-15.
16. Van de Berg, W.D., et al., *Perinatal asphyxia induced neuronal loss by apoptosis in the neonatal rat striatum: a combined TUNEL and stereological study*. Exp Neurol, 2002. **174**(1): p. 29-36.
17. Gunn, A.J., *Cerebral hypothermia for prevention of brain injury following perinatal asphyxia*. Curr Opin Pediatr, 2000. **12**(2): p. 111-5.
18. Delivoria-Papadopoulos, M. and O.P. Mishra, *Mechanisms of perinatal cerebral injury in fetus and newborn*. Ann N Y Acad Sci, 2000. **900**: p. 159-68.
19. Mishra, O.P. and M. Delivoria-Papadopoulos, *Cellular mechanisms of hypoxic injury in the developing brain*. Brain Res Bull, 1999. **48**(3): p. 233-8.
20. Kohlhauser, C., et al., *Cholinergic, monoaminergic and glutamatergic changes following perinatal asphyxia in the rat*. Cell Mol Life Sci, 1999. **55**(11): p. 1491-501.

21. Arundine, M. and M. Tymianski, *Molecular mechanisms of calcium-dependent neurodegeneration in excitotoxicity*. Cell Calcium, 2003. **34**(4-5): p. 325-37.
22. Creagh, E.M., H. Conroy, and S.J. Martin, *Caspase-activation pathways in apoptosis and immunity*. Immunol Rev, 2003. **193**: p. 10-21.
23. Northington, F.J., et al., *Early Neurodegeneration after Hypoxia-Ischemia in Neonatal Rat Is Necrosis while Delayed Neuronal Death Is Apoptosis*. Neurobiol Dis, 2001. **8**(2): p. 207-19.
24. Masliah, E., et al., *Quantitative synaptic alterations in the human neocortex during normal aging*. Neurology, 1993. **43**(1): p. 192-7.
25. Wong, T.P., et al., *Synaptic numbers across cortical laminae and cognitive performance of the rat during ageing*. Neuroscience, 1998. **84**(2): p. 403-12.
26. Stroemer, R.P., T.A. Kent, and C.E. Hulsebosch, *Increase in synaptophysin immunoreactivity following cortical infarction*. Neurosci Lett, 1992. **147**(1): p. 21-4.
27. Akulinin, V.A., et al., *Dendritic changes of the pyramidal neurons in layer V of sensory-motor cortex of the rat brain during the postresuscitation period*. Resuscitation, 1997. **35**(2): p. 157-64.
28. Horner, C.H., H.A. Davies, and M.G. Stewart, *Hippocampal synaptic density and glutamate immunoreactivity following transient cerebral ischaemia in the chick*. Eur J Neurosci, 1998. **10**(12): p. 3913-7.
29. Stepanov, S.S., et al., *An ultrastructural study into the effect of global transient cerebral ischaemia on the synaptic population of the cerebellar cortex in rats*. Resuscitation, 1998. **39**(1-2): p. 99-106.
30. Loidl, C.F., et al., *Long-term effects of perinatal asphyxia on basal ganglia neurotransmitter systems studied with microdialysis in rat*. Neurosci Lett, 1994. **175**(1-2): p. 9-12.
31. Chen, Y., et al., *Perinatal asphyxia induces long-term changes in dopamine D1, D2, and D3 receptor binding in the rat brain*. Exp Neurol, 1997. **146**(1): p. 74-80.
32. Gross, J., et al., *Effect of perinatal asphyxia on tyrosine hydroxylase and D2 and D1 dopamine receptor mRNA levels expressed during early postnatal development in rat brain*. Brain Res Mol Brain Res, 2005. **134**(2): p. 275-81.
33. Cowan, D.B., et al., *Hypoxia and stretch regulate intercellular communication in vascular smooth muscle cells through reactive oxygen species formation*. Arterioscler Thromb Vasc Biol, 2003. **23**(10): p. 1754-60.
34. Sargent, M.A., et al., *Cerebellar vermian atrophy after neonatal hypoxic-ischemic encephalopathy*. AJNR Am J Neuroradiol, 2004. **25**(6): p. 1008-15.
35. Niermeyer, S., et al., *Resuscitation of newborns*. Ann Emerg Med, 2001. **37**(4 Suppl): p. S110-25.
36. Dammann, O. and A. Leviton, *Brain damage in preterm newborns: biological response modification as a strategy to reduce disabilities*. J Pediatr, 2000. **136**(4): p. 433-8.
37. Gluckman, P.D., C.S. Pinal, and A.J. Gunn, *Hypoxic-ischemic brain injury in the newborn: pathophysiology and potential strategies for intervention*. Semin Neonatol, 2001. **6**(2): p. 109-20.
38. Volpe, J.J., *Perinatal brain injury: from pathogenesis to neuroprotection*. Ment Retard Dev Disabil Res Rev, 2001. **7**(1): p. 56-64.
39. Gluckman, P.D., et al., *Selective head cooling with mild systemic hypothermia after neonatal encephalopathy: multicentre randomised trial*. Lancet, 2005. **365**(9460): p. 663-70.
40. Shankaran, S., et al., *Whole-body hypothermia for neonates with hypoxic-ischemic encephalopathy*. N Engl J Med, 2005. **353**(15): p. 1574-84.
41. Cai, Z., J.D. Fratkin, and P.G. Rhodes, *Prenatal ischemia reduces neuronal injury caused by neonatal hypoxia-ischemia in rats*. Neuroreport, 1997. **8**(6): p. 1393-8.

42. Andoh, T., P.B. Chock, and C.C. Chiueh, *Preconditioning-mediated neuroprotection: role of nitric oxide, cGMP, and new protein expression*. *Ann N Y Acad Sci*, 2002. **962**: p. 1-7.
43. Stenzel-Poore, M.P., et al., *Effect of ischaemic preconditioning on genomic response to cerebral ischaemia: similarity to neuroprotective strategies in hibernation and hypoxia-tolerant states*. *Lancet*, 2003. **362**(9389): p. 1028-37.
44. Tanaka, H., et al., *Ischemic preconditioning acts upstream of GluR2 down-regulation to afford neuroprotection in the hippocampal CA1*. *Proc Natl Acad Sci U S A*, 2002. **99**(4): p. 2362-7.
45. Dawson, V.L. and T.M. Dawson, *Neuronal ischaemic preconditioning*. *Trends Pharmacol Sci*, 2000. **21**(11): p. 423-4.
46. Chang, Y.C. and C.C. Huang, *Perinatal brain injury and regulation of transcription*. *Curr Opin Neurol*, 2006. **19**(2): p. 141-7.
47. Gidday, J.M., et al., *Neuroprotection from ischemic brain injury by hypoxic preconditioning in the neonatal rat*. *Neurosci Lett*, 1994. **168**(1-2): p. 221-4.
48. Gustavsson, M., et al., *Hypoxic preconditioning confers long-term reduction of brain injury and improvement of neurological ability in immature rats*. *Pediatr Res*, 2005. **57**(2): p. 305-9.
49. Xiao, F., et al., *Reduced nitric oxide is involved in prenatal ischemia-induced tolerance to neonatal hypoxic-ischemic brain injury in rats*. *Neurosci Lett*, 2000. **285**(1): p. 5-8.
50. Vannucci, R.C., J. Towfighi, and S.J. Vannucci, *Hypoxic preconditioning and hypoxic-ischemic brain damage in the immature rat: pathologic and metabolic correlates*. *J Neurochem*, 1998. **71**(3): p. 1215-20.
51. Ran, R., et al., *Hypoxia preconditioning in the brain*. *Dev Neurosci*, 2005. **27**(2-4): p. 87-92.
52. Sharp, F.R., et al., *Hypoxic preconditioning protects against ischemic brain injury*. *NeuroRx*, 2004. **1**(1): p. 26-35.
53. Bernaudin, M., et al., *Brain genomic response following hypoxia and re-oxygenation in the neonatal rat. Identification of genes that might contribute to hypoxia-induced ischemic tolerance*. *J Biol Chem*, 2002. **277**(42): p. 39728-38.
54. Johnston, M.V., *Excitotoxicity in perinatal brain injury*. *Brain Pathol*, 2005. **15**(3): p. 234-40.
55. Cavalieri, B., *Geometria indivisibilibus continuorum. Bononiae: Typis Clementis Ferronij*. 1635: Unione Tipografico-Editrice Torinese.
56. Schmitz, C. and P.R. Hof, *Design-based stereology in neuroscience*. *Neuroscience*, 2005. **130**(4): p. 813-31.
57. Rutten, B.P., et al., *Age-related loss of synaptophysin immunoreactive presynaptic boutons within the hippocampus of APP751SL, PS1M146L, and APP751SL/PS1M146L transgenic mice*. *Am J Pathol*, 2005. **167**(1): p. 161-73.
58. El-Khodori, B.F. and P. Boksa, *Differential vulnerability of male versus female rats to long-term effects of birth insult on brain catecholamine levels*. *Exp Neurol*, 2003. **182**(1): p. 208-19.
59. Tanila, H., et al., *Effect of sex and age on brain monoamines and spatial learning in rats*. *Neurobiol Aging*, 1994. **15**(6): p. 733-41.
60. Zhang, Y.Q., et al., *Effects of gender and estradiol treatment on focal brain ischemia*. *Brain Res*, 1998. **784**(1-2): p. 321-4.
61. Dobbing, J. and J. Sands, *Quantitative growth and development of human brain*. *Arch Dis Child*, 1973. **48**(10): p. 757-67.
62. Engert, F. and T. Bonhoeffer, *Dendritic spine changes associated with hippocampal long-term synaptic plasticity*. *Nature*, 1999. **399**(6731): p. 66-70.

63. Yang, S.N., et al., *Impaired SynGAP expression and long-term spatial learning and memory in hippocampal CA1 area from rats previously exposed to perinatal hypoxia-induced insults: beneficial effects of A68930*. *Neurosci Lett*, 2004. **371**(1): p. 73-8.
64. Ramirez, M.R., et al., *Neonatal hypoxia-ischemia reduces ganglioside, phospholipid and cholesterol contents in the rat hippocampus*. *Neurosci Res*, 2003. **46**(3): p. 339-47.
65. Adams, I. and D.G. Jones, *Quantitative ultrastructural changes in rat cortical synapses during early-, mid- and late-adulthood*. *Brain Res*, 1982. **239**(2): p. 349-63.
66. Fiala, J.C., J. Spacek, and K.M. Harris, *Dendritic spine pathology: cause or consequence of neurological disorders?* *Brain Res Brain Res Rev*, 2002. **39**(1): p. 29-54.
67. Jacobs, B. and A.B. Scheibel, *A quantitative dendritic analysis of Wernicke's area in humans. I. Lifespan changes*. *J Comp Neurol*, 1993. **327**(1): p. 83-96.
68. Hinds, J.W. and N.A. McNelly, *Aging of the rat olfactory bulb: growth and atrophy of constituent layers and changes in size and number of mitral cells*. *J Comp Neurol*, 1977. **72**(3): p. 345-67.
69. Horn, D., N. Levy, and E. Ruppin, *Neuronal-based synaptic compensation: a computational study in Alzheimer's disease*. *Neural Comput*, 1996. **8**(6): p. 1227-43.
70. Cantagrel, S., et al., *Hypoxic preconditioning reduces apoptosis in a rat model of immature brain hypoxia-ischaemia*. *Neurosci Lett*, 2003. **347**(2): p. 106-10.
71. Zhao, P. and Z. Zuo, *Prenatal hypoxia-induced adaptation and neuroprotection that is inducible nitric oxide synthase-dependent*. *Neurobiol Dis*, 2005. **20**(3): p. 871-80.
72. Eisen, A., et al., *Ischemic preconditioning: nearly two decades of research. A comprehensive review*. *Atherosclerosis*, 2004. **172**(2): p. 201-10.
73. Dirnagl, U., R.P. Simon, and J.M. Hallenbeck, *Ischemic tolerance and endogenous neuroprotection*. *Trends Neurosci*, 2003. **26**(5): p. 248-54.
74. Bergeron, M., et al., *Role of hypoxia-inducible factor-1 in hypoxia-induced ischemic tolerance in neonatal rat brain*. *Ann Neurol*, 2000. **48**(3): p. 285-96.
75. Bond, A., et al., *NMDA receptor antagonism, but not AMPA receptor antagonism attenuates induced ischaemic tolerance in the gerbil hippocampus*. *Eur J Pharmacol*, 1999. **380**(2-3): p. 91-9.
76. Gonzalez-Zulueta, M., et al., *Requirement for nitric oxide activation of p21(ras)/extracellular regulated kinase in neuronal ischemic preconditioning*. *Proc Natl Acad Sci U S A*, 2000. **97**(1): p. 436-41.
77. Chen, J., et al., *Suppression of endogenous bcl-2 expression by antisense treatment exacerbates ischemic neuronal death*. *J Cereb Blood Flow Metab*, 2000. **20**: p. 1033-1039.
78. Lee, H.T., et al., *cAMP response element-binding protein activation in ligation preconditioning in neonatal brain*. *Ann Neurol*, 2004. **56**(5): p. 611-23.
79. Kapinya, K.J., K. Prass, and U. Dirnagl, *Isoflurane induced prolonged protection against cerebral ischemia in mice: a redox sensitive mechanism?* *Neuroreport*, 2002. **13**(11): p. 1431-5.
80. Kersten, J.R., et al., *Isoflurane mimics ischemic preconditioning via activation of K(ATP) channels: reduction of myocardial infarct size with an acute memory phase*. *Anesthesiology*, 1997. **87**(2): p. 361-70.
81. Venerosi, A., et al., *C-section birth per se or followed by acute global asphyxia altered emotional behaviour in neonate and adult rats*. *Behav Brain Res*, 2006. **168**(1): p. 56-63.

Appendix

Appendix 1: Results of behavioral testing of the severe fetal asphyctic animals

In summary, the results of the behavioral testing (previously done within this group) of the same sFA animals as used in this study are as follows. Cognitive performance was assessed using the spatial Morris Water Maze (MWM) task at 1.5, 6, 12 and 19 months. The total distance moved to reach the platform provides a measure for the ability to learn a task. The data of those distances are presented in figure 1 of this appendix. Both groups had acquired the task as shown by the decrease in distance moved between the first and the second trial. Animals of both groups had also no problem remembering the task at 1.5, 6 and 12 months, which is presented in the figure by the low values at the 3rd and 4th trial. At 19 months, however, asphyctic animals did have problems remembering the task compared to the sham animals. The distances moved during the 3rd and 4th trial were significantly higher in the asphyctic group.

Morris Water Maze Testing

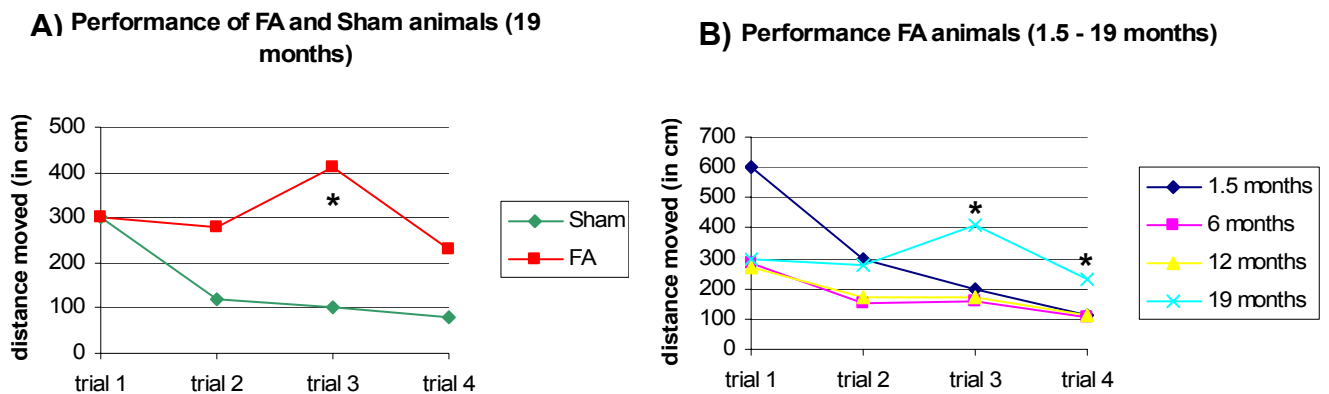


Figure 1: The results of the Morris Water Maze testing. (A) The results of the sFA and the Sham group at the age of 19 months. During the 3rd trial, the FA animals had a problem remembering the location of the platform. (B) The results of the FA animals at the age of 1.5, 6, 12 and 19 months, showing that only the aged animals significantly performed less during the 3rd and 4th trial. (* $P < 0,05$) (sFA = severe fetal asphyxia)

Locomotor activity and anxiety-related behavior were analyzed at 6 and 19 months using the open field test (OF). Figure 3 in this appendix depicts the results. The asphyctic rats showed no differences compared to the sham-operated rats at 6 months. Though at 19 months, the asphyctic rats spent significantly more time in the corners and less time along the walls and in the center. These observations point towards anxious behavior. There was also a significant difference in the total distance moved, indicating that the asphyctic rats are less active.

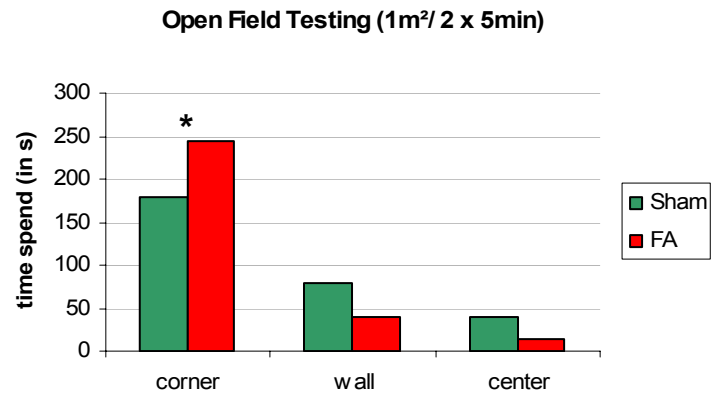


Figure 2: The results of the Open Field testing of the sFA and sham animals at the age of 19 months. The sFA animals spent significantly more time in the corners compared to the sham animals. The sham animals, in contrast, spend more time in the center area. (* $P < 0,05$) (sFA = severe fetal asphyxia)

Auteursrechterlijke overeenkomst

Opdat de Universiteit Hasselt uw eindverhandeling wereldwijd kan reproduceren, vertalen en distribueren is uw akkoord voor deze overeenkomst noodzakelijk. Gelieve de tijd te nemen om deze overeenkomst door te nemen en uw akkoord te verlenen.

Ik/wij verlenen het wereldwijde auteursrecht voor de ingediende eindverhandeling:

Fetal asphyxia: short and long-term consequences and its role in preconditioning

Richting: **Master in de biomedische wetenschappen**

Jaar: **2006**

in alle mogelijke mediaformaten, - bestaande en in de toekomst te ontwikkelen - , aan de Universiteit Hasselt.

Deze toekenning van het auteursrecht aan de Universiteit Hasselt houdt in dat ik/wij als auteur de eindverhandeling, - in zijn geheel of gedeeltelijk -, vrij kan reproduceren, (her)publiceren of distribueren zonder de toelating te moeten verkrijgen van de Universiteit Hasselt.

U bevestigt dat de eindverhandeling uw origineel werk is, en dat u het recht heeft om de rechten te verlenen die in deze overeenkomst worden beschreven. U verklaart tevens dat de eindverhandeling, naar uw weten, het auteursrecht van anderen niet overtreedt.

U verklaart tevens dat u voor het materiaal in de eindverhandeling dat beschermd wordt door het auteursrecht, de nodige toelatingen hebt verkregen zodat u deze ook aan de Universiteit Hasselt kan overdragen en dat dit duidelijk in de tekst en inhoud van de eindverhandeling werd genotificeerd.

Universiteit Hasselt zal u als auteur(s) van de eindverhandeling identificeren en zal geen wijzigingen aanbrengen aan de eindverhandeling, uitgezonderd deze toegelaten door deze licentie

Ik ga akkoord,

Eveline STRACKX

Datum: